Molina Puerto, J.; Fernández Sáez, J.; Del Río García, AI.; Bonastre Cano, JA.; Cases Iborra, FJ. (2011). Electrochemical synthesis of polyaniline on conducting fabrics of polyester covered with polypyrrole/PW12O403-. Chemical and electrochemical characterization. Synthetic Metals. 161(11-12):953-963. doi:10.1016/j.synthmet.2011.02.029.

Highlighted

Electrochemical synthesis of polyaniline on conducting fabrics of polyester covered with polypyrrole/$PW_{12}O_{40}^{3-}$. Chemical and electrochemical characterization.

J. Molina, J. Fernández, A.I. del Río, J. Bonastre, F. Cases *

Departamento de Ingeniería Textil y Papelera, EPS de Alcoy, Universidad Politécnica de Valencia, Plaza Ferrándiz y Carbonell s/n, 03801 Alcoy, Spain

Abstract

Polyaniline (Pani) has been electrochemically polymerized on conducting fabrics of polyester covered with polypyrrole/$PW_{12}O_{40}^{3-}$, obtaining a double conducting polymer layer. Electrochemical synthesis was performed by potentiostatic synthesis at 1 V. The chemical characterization of the material before and after Pani polymerization was performed by means of X-ray photoelectron spectroscopy (XPS), energy dispersive X-ray (EDX) and Fourier transform infrared spectroscopy (FTIR). The morphology of the coatings was observed employing scanning electron microscopy (SEM). The electrochemical characterization was performed by cyclic voltammetry (CV) and scanning electrochemical microscopy (SECM). It has been demonstrated that scan rate is an important parameter that influences the response obtained when characterizing conducting fabrics by CV. High scan rates do not allow the observation of redox peaks. However if lower scan rates are employed its apparition has been reported. The electrochemical deposit of polyaniline enhances the electroactivity of the material as it has been demonstrated by CV. SECM measurements showed local response with positive feedback (electroactive material) for the samples in open circuit conditions.

XPS analysis also showed a higher doping level (N^+/N), consistent with higher material electroactivity.

Keywords: Polyaniline, polypyrrole, conducting fabrics, cyclic voltammetry, SECM.

---

* Corresponding author. Fax.: +34 96 652 8438

E-mail address: fjcases@txp.upv.es (Prof. F. Cases)

1. Introduction

The production of textiles with new properties, such as conductivity, is a new field being investigated. The employment of conducting polymers is one of the methods that have been used to achieve this purpose. Polypyrrole (Ppy) has been the most employed conducting polymer when producing conducting fabrics [1-8]. The chemical polymerization of pyrrole in the presence of textile substrates produces a layer of conducting polymer on the fabrics. Applications of conducting polymers coated textiles are varied and numerous; like antistatic materials [1], gas sensors [2], biomechanical sensors [3], electrotherapy [4], heating devices [5-7] or microwave attenuation [8]. Another suitable method to produce conducting textiles is the electrochemical deposition of conducting polymers. The electrochemical polymerization is a more controlled method that only produces the conducting polymer on the surface of the desired electrode. The electrochemical polymerization can be performed indirectly or directly depending on the conductivity of the substrate employed as electrode. If the substrate is insulating, only an indirect electrochemical deposition can be performed.

Only few papers related to this topic can be seen in bibliography and the majority of them perform an indirect electrochemical deposition [9-12].

One of the applications that our group aims to is the employment of conducting fabrics in catalysis, or as a support with high surface area to electrodeposit Pt nanoparticles and enhance its electroactivity [13,14]. For instance, conducting polymers have been employed in environmental applications; electrodes modified with conducting polymers have been used in Cr^{6+} (toxic) reduction to Cr^{3+} (not toxic) [15] or nitrites electroreduction [16]. The employment of polypyrrole coated textiles in the electrochemical removal of the textile dye C. I. Direct Red 80 has also been reported [17]. Polyaniline/MnO_2 catalyst and H_2O_2 as an oxidant have been employed in the degradation of organic dyes such as Direct Red 81, Indigo Carmine and Acid Blue 92 [18,19].

In the present paper conducting textiles of polyester (PES) covered with polypyrrole/$PW_{12}O_{40}^{3-}$ have been produced to obtain a conducting substrate. Once the substrate was conductive, a direct electrochemical deposition of polyaniline was performed. In the end a double conducting polymer layer of polypyrrole/polyaniline was obtained. Chemical characterization of the conducting fabrics was done by XPS, EDX and FTIR-ATR; morphological characterization was done by means of SEM. The electrochemical and electrocatalytic properties of the monolayer and bilayer films have been measured by means of cyclic voltammetry (CV) and scanning electrochemical microscopy (SECM). In bibliography only a few assays of CV have been performed on conducting textiles [20,21]. In the present paper it is reported the influence of the scan rate in the characterization of conducting fabrics. The electroactivity of the samples was measured by scanning electrochemical microscopy (SECM). SECM is a relatively novel

(1989) and powerful technique that is becoming more popular among researchers [22-24]. Its employment in conducting fabrics has not been reported to our knowledge since the most employed substrate in bibliography is Pt.

2. Experimental

2.1. Reagents and materials

Analytical grade pyrrole, aniline, ferric chloride, sulphuric acid, sodium sulphate, sodium dihydrogenophosphate, disodium hydrogenophosphate and sodium hydroxide were provided by Merck. Normapur acetone was acquired from Prolabo. Analytical grade phosphotungstic acid hydrate was supplied by Fluka. Hexaammineruthenium (III) choride ($Ru(NH_3)_6Cl_3$) and potassium chloride were used as received from Acros Organics and Scharlau respectively. Solutions were deoxygenated by bubbling nitrogen (N_2 premier X50S). Ultrapure water was obtained from an Elix 3 Millipore-Milli-Q Advantage A10 system with a resistivity near to 18.2 MΩ cm.

Aniline was purified by distillation before use. Distillation was performed at reduced pressure in order to avoid thermal degradation of the monomer. After distillation aniline was stored in the dark at 0 ºC.

Polyester textile was acquired from Viatex S.A. and their characteristics were: fabric surface density, 140 g m^{-2}; warp threads per cm, 20 (warp linear density, 167 dtex); weft threads per cm, 60 (weft linear density, 500 dtex). These are specific terms used in the field of textile industry and their meaning can be consulted in a textile glossary [25].

2.2. Chemical synthesis of PPy/$PW_{12}O_{40}^{3-}$ on polyester fabrics

Chemical synthesis of PPy on polyester fabrics was done as reported in our previous study [26]. The size of the samples was 6 cm x 6 cm approximately. Previously to reaction, polyester was degreased with acetone in ultrasound bath and washed with water. Pyrrole concentration employed was 2 g l^{-1} and the molar relations of reagents employed in the chemical synthesis bath were pyrrole: $FeCl_3$: $H_3PW_{12}O_{40}$ (1: 2.5: 0.2). The next stage was the adsorption of pyrrole and counter ion ($PW_{12}O_{40}^{3-}$) (V=200 ml) on the fabric for 30 min in an ice bath without stirring. At the end of this time, the $FeCl_3$ solution (V=50 ml) was added and oxidation of the monomer took place during 150 min without stirring. Adsorption and reaction were performed in a precipitation beaker. The conducting fabric was washed with water to remove PPy not joined to fibers. The conducting fabric was dried in a desiccator for at least 24 h before measurements. The weight increase was measured obtaining a value around 10 %.

2.3. Electrochemical synthesis of Pani on conducting fabrics of PES-PPy/$PW_{12}O_{40}^{3-}$

Electrosynthesis of Pani on the fabrics of PES-PPy/$PW_{12}O_{40}^{3-}$ was performed using an Autolab PGSTAT302 potentiostat/galvanostat (Ecochemie). All electrochemical experiments were carried out at room temperature and without stirring. The counter electrodes (CE) were made of stainless steel. The working electrode (WE) was made cutting a strip of the conducting fabric (PES-PPy/$PW_{12}O_{40}^{3-}$) and locating it between two Titanium plates. Potential measurements were referred to Ag/AgCl (3 M KCl) reference electrode. Oxygen was removed from solution by bubbling nitrogen gas.

The conducting fabrics have an ohmic potential drop that needs to be compensated; otherwise the measured potentials will not be real. Therefore, the ohmic potential drop was measured and entered in the Autolab software.

The electrochemical synthesis of polyaniline was performed in 0.5 M H_2SO_4 and 0.5 M aniline aqueous solution, in N_2 atmosphere. The conducting fabric electrode was soaked with the solution to allow the diffusion of the monomer to the textile electrode. The method of synthesis employed was the potentiostatic synthesis. The synthesis potential for the potentiostatic synthesis was determined using cyclic voltammetry measurements; 1 V was selected as an adequate potential for the potentiostatic synthesis. For the potentiostatic synthesis, the potential was risen up from open circuit potential (ocp) of the electrode to 1 V. The electrosynthesis continued during the necessary time to achieve the desired electrical charge (C cm^{-2}).

2.4. FTIR-ATR spectroscopy

Fourier transform infrared spectroscopy with horizontal multirebound attenuated total reflection (FTIR-ATR) was performed with a Nicolet 6700 Spectrometer equipped with DTGS detector. An accessory with pressure control was employed to equalize the pressure in the different solid samples. A prism of ZnSe was employed. Spectra were collected with a resolution of 4 cm^{-1} and 100 scans were averaged for each sample.

2.5. X-Ray photoelectron spectroscopy

XPS analyses were conducted at a base pressure of at $5 \cdot 10^{-10}$ mbars and a temperature around 173 K. The XPS spectra were obtained with a VG-Microtech Multilab electron spectrometer by using unmonochromatized Mg K_α (1253.6 eV) radiation from a twin anode source operating at 300 W (20 mA, 15 KV). The binding energy (BE) scale was calibrated with reference to the C_{1s} line at 284.6 eV. The C1s, O1s and N1s core levels

spectra were analyzed for the sample of PES-PPy/$PW_{12}O_{40}^{3-}$ and the sample of PES-PPy/$PW_{12}O_{40}^{3-}$ + Pani.

2.6. SEM and EDX characterization

A Jeol JSM-6300 scanning electron microscope was employed to observe the morphology of the samples and perform EDX analyses. SEM analyses were performed using an acceleration voltage of 20 kV. EDX measurements were done between 0 and 20 keV.

2.7. Cyclic voltammetry measurements

An Autolab PGSTAT302 potentiostat/galvanostat was employed to perform CV measurements in the different pH solutions: pH~0 (0.5 M H_2SO_4), pH~0.7 (0.1 M H_2SO_4), pH~7 (NaH_2PO_4-NaH_2PO_4 buffer and Na_2SO_4 0.1 M), pH~13 (0.1 M NaOH and 0.1 M Na_2SO_4). Measurements were done at room temperature and without stirring. The CE employed was made of stainless steel; the pre-treatment consisted on polishing, degreasing with acetone in an ultrasonic bath and washing with water in the ultrasonic bath. The WE was made by cutting a strip of the conducting textile of PPy or the conducting textile of PPy covered with Pani. The sample was located between two Ti plates to perform the measurements. Potential measurements were referred to Ag/AgCl (3 M KCl) reference electrode. Oxygen was removed from solution by bubbling nitrogen gas for 10 min and then a N_2 atmosphere was maintained during the measurements. The ohmic potential drop was measured and introduced in the Autolab software. For the sample of PES-PPy/$PW_{12}O_{40}^{3-}$, the measurements were done between -0.4 V and +0.4 V. For the sample containing Pani, the potential range employed was -

0.2 V, +0.7 V. The characterization by means of CV has been done at different scan rates as it was corroborated the influence of this parameter on the electrochemical response obtained. The scan rates employed were 50 mV s^{-1}, 5 mV s^{-1} and 1 mV s^{-1}.

2.8. SECM measurements

SECM measurements were carried out with a scanning electrochemical microscope of Sensolytics. The three-electrode cell configuration consisted of a 100-μm-diameter Pt ultra-microelectrode (UME) working electrode, a Pt wire auxiliary electrode and an Ag/AgCl (3 M KCl) reference electrode. The solution selected for this study was 0.01 M $Ru(NH_3)_6Cl_3$ in aqueous 0.1 M KCl supporting electrolyte. All the experiments were carried out in inert nitrogen atmosphere. PES, PES-PPy/$PW_{12}O_{40}^{3-}$ and PES-PPy/$PW_{12}O_{40}^{3-}$ + Pani (1.5 C cm^{-2}) (0.25 cm^2 geometrical area) were chosen as substrates for the SECM measurements. The substrates were glued with epoxy resin on glass microscope slides.

The positioning of the Pt UME tip was achieved by first carefully putting it in contact with the substrate surface and then moving it in z direction (height of the electrode). Once the electrode was at the desired height, the electrode was approached to the substrate surface; the current of the UME was recorded to obtain the approach curves. Approach curves give us an indication of the electroactivity of the surface.

The surfaces were also scanned at their open circuit potential (OCP), and hence, the potential of the substrate was controlled indirectly by the redox couple concentration. Scanning the surface of the fabrics, a topographic profile of the sample was obtained.

3. Results and discussion

3.1. Electrochemical synthesis of Pani on PES-PPy/$PW_{12}O_{40}^{3-}$

The synthesis potential for the potentiostatic synthesis was established by cyclic voltammetry measurements (Fig. 1). The cyclic voltammetry measurements were carried out in the same conditions than the potentiostatic synthesis (0.5 M aniline and 0.5 M H_2SO_4). The potential was varied between -0.2 V and 1.1 V with a scan rate of 5 mV s^{-1}, 5 scans were registered. It can be seen that the current density grows with the number of scan, indicating that the Pani synthesis was being carried out. The potential of 1 V was selected as an adequate potential to carry out the potentiostatic synthesis because beyond this potential, the current density begin to grow sharply. As it will be explained later, at this potential overoxidation was not observed by means of XPS analyses.

3.2. XPS measurements

The C1s, O1s and N1s core levels spectra were analyzed for the sample of PES-PPy/$PW_{12}O_{40}^{3-}$ and the sample of PES-PPy/$PW_{12}O_{40}^{3-}$ covered with Pani. Table 1 shows chemical composition and doping ratio obtained by N analysis (N^+/N ratio) for both samples. The sample covered with Ppy/$PW_{12}O_{40}^{3-}$ should ideally have the formula $C_4H_3N(PW_{12}O_{40}^{3-})_x$, where "x" is the fractional doping level obtained by W analysis. XPS analysis showed a systematic carbon excess, which may be due to surface hydrocarbon contamination [27]. The composition analysis also showed an oxygen excess. This may be due to PPy ring oxidation attributed to PPy reaction with water as synthesis solvent [28]. The doping ratio obtained by nitrogen analysis, was in good agreement with the fractional doping level performed by tungsten analysis. The doping

ratio represented by the (N^+/N_{Total}) ratio was found to be 19.6%. As $PW_{12}O_{40}^{3-}$ presents 3 negative charges per molecule, the $PW_{12}O_{40}^{3-}$ fractional doping level would be 0.0196/3 = 0.065, close to 0.053 obtained by W analysis. For the sample covered with Pani/HSO_4^-/SO_4^{2-} there was a considerable difference between doping ratio estimated by atomic ratio N^+/N_{Total}, and doping level obtained by atomic ratio S/N. This discrepancy can be attributed to covalently bound sulfur bonds [29]. Covalently bound sulfur bonds belong to the polymeric structure, but they do not need positive charged nitrogen as polarons or bipolarons to accomplish the electroneutrality principle. So, the N^+ could be lower due to a minor number of polaronic sites. Table 2 shows the C1s, O1s, N1s core level binding energies assignments for the samples analyzed.

3.2.1. C1s analysis.

Fig. 2-a shows the deconvoluted high resolution C1s spectrum for the sample of PES-PPy/$PW_{12}O_{40}^{3-}$. Three peaks appear at the following binding energies: 284.1, 285.6 and 287.4 eV. The component at the lowest binding energy is due to C-C/C-H groups. The peak at 285.6 eV is assigned to C-N groups in the pyrrole rings [30-32]. The binding energy peak at 287.4 eV is ascribed to carbonyl C=O groups [33,34]. The appearance of C=O groups is mainly due to the presence of pyrrole overoxidation during chemical polymerization in aqueous media, as commented before. It has been proved that the polypyrrole is simultaneously degraded during the synthesis in short soluble maleimide molecules. This degradation process may be attributed to the polymer overoxidation which is described as a gradual polymer oxidation by water in the presence of $FeCl_3$. Quantitative measurements confirm that polymerization is second-order kinetics with respect to $FeCl_3$ while overoxidation appears to be only first order [28]. Contamination

with particulated PPy might also be on the surface due to the formation of aggregates and individual particles of colloidal PPy [35]. Fig. 2-a shows that C-C/C-H peak area is significantly greater than C-N one. For the pyrrole structure, the atomic ratio (C-C/C-H)/C-N must be equal to 1.0. The higher C-C/C-H contribution is coherent with a maleimide-like structure where C=O groups appears at α positions (C-N groups). This overoxidation might be roughly estimated as the atomic ratio $C{=}O/C_{Total}$, obtaining a value around 8 %. As surface hydrocarbon contamination may be present, this is a minimum value.

For the sample covered with Pani, Fig. 2-b shows two binding energy values for C1s core level at 284.2 and 285.8 eV. These contributions are related to C-C/C-H and C-N groups of the aniline ring, respectively. Peak corresponding to C=O group did not appear in the XPS analysis; so overoxidation was not present in the polyaniline layer. For this reason, the synthesis potential of 1 V was an adequate potential to perform the electrochemical synthesis as it was explained previously.

3.2.2. O1s analysis.

Fig. 2-c shows the high resolution O1s spectrum for the sample of PES-PPy/$PW_{12}O_{40}^{3-}$. The O1s core level peak was deconvoluted in two contributions centered at 530.3 and 531.7 eV. These contributions are assigned to W-O-W groups and W=O groups in the $PW_{12}O_{40}^{3-}$ counter ion respectively [36]. In Fig 2-d the high resolution O1s core level spectrum for the sample covered with Pani can be observed. The spectrum was deconvoluted in two peaks at 531.2 and 532.8 eV. These binding energies were assigned to SO_4^{2-} and HSO_4^- respectively [37], and are due to incorporated counter ion within the polymer. The proportion between HSO_4^-/SO_4^{2-} molecules was 1/3. Although

the low pH of the sulfuric synthesis solution might indicate a major amount of HSO_4^- as counterion, it is important to take into account that Pani is protonated in acid media [38], being able to displace the HSO_4^-/SO_4^{2-} equilibrium, pK_a=1.9 [39], to the formation of SO_4^{2-}.

3.2.3. N1s analysis.

Fig. 2-e shows the high resolution N1s spectrum for the sample of PES-PPy/$PW_{12}O_{40}^{3-}$. The N1s spectrum was deconvoluted into two contributions, centered at 399.7 and 401.9 eV. The peak at 399.7 eV was assigned to the neutral amine-like (–NH–) structure ~~which is characteristic of pyrrolylium nitrogen~~ [30,33,40]. The peak at 401.9 eV was attributed to bipolaronic positively charged nitrogen, $=NH^+$ or N^{2+}. The electron-deficient nitrogen species arise from delocalization of electron density from the polypyrrole ring as a result of the formation of electronic defects (bipolarons) [31,40]. The doping ratio represented by the (N^{2+}/N_{Total}) ratio was found to be 19.6 %. Fig. 2-f shows the high resolution N1s spectrum for sample covered with Pani. The spectrum was deconvoluted in three peaks centered at 398.8, 399.7 and 401.6 eV. The first peak at 398.8 eV was attributed to deprotonated, uncharged, imine-like nitrogens (>C=N-) [30, 41-43]. The peak at 399.7 eV was assigned to the neutral amine-like (–NH–) structure. The peak at 401.6 eV was attributed to nitrogen atoms with a single positive charge, polaronic nitrogen N^+ [31]. The doping ratio (N^+/N_{Total}) was 22.4 %. The atomic ratios (>C=N-)/N_{Total} and (-NH)/N_{Total} were 31.5 and 46.1 %, respectively. The sum of atomic ratios for imine-like nitrogen and polaronic nitrogen was 53.9 %. This value is near to 50 % of an ideal intrinsically oxidized emeraldine structure [38]. These results confirm that conducting textiles covered with Pani were predominantly obtained in the

emeraldine form. As it can be seen in Table 1, when the electrochemical polymerization of polyaniline was performed, the doping ratio suffered a noticeable increase.

3.3. SEM and EDX measurements

In Fig. 3-a it can be seen the micrograph of the sample of PES-PPy/$PW_{12}O_{40}^{3-}$. As it can be observed, the whole fabric is covered by a layer of PPy/$PW_{12}O_{40}^{3-}$. The presence of polypyrrole aggregates is also noticeable. When the electrochemical synthesis of Pani was carried out, the entire surface of the fabric was covered by polyaniline. In Fig. 3-b it is shown a micrograph of the sample covered with Pani (35 C cm^{-2}) at low magnification (100x). The fibers of the fabric could hardly be observed as Pani had grown on the surface of the fibers and between the interstices of the fibers. In Fig. 3-c it is shown a zone where Pani was grown on the surface of the fibers. If Fig. 3-a and 3-c are compared, it can be observed the formation of a globular deposit on the surface of the fabric fibers. Micrograph in Fig. 3-d has been enhanced to observe better the deposit morphology. As it can be seen, Pani deposit presents a globular morphology. Similar morphology has been obtained when Pani was deposited by potentiostatic method on Al-Pt electrode [44]. The morphology of the Pani deposits depends on various factors, such as: polymerization conditions, synthesis technique, acid employed as electrolyte, etc [45,46].

EDX analyses were also performed to observe zonal composition in the samples analyzed. The EDX spectrum of the PES-PPy/$PW_{12}O_{40}^{3-}$ sample (Fig. 4-a) showed the presence of W, this indicates that the counter ion ($PW_{12}O_{40}^{3-}$) has been incorporated in the polypyrrole structure. The presence of Fe and Cl arise from the use of $FeCl_3$ as oxidant in polypyrrole synthesis. A zonal analysis was done on the surface of a fiber

covered with polyaniline (Fig. 4-b). The presence of S indicates the growth of the Pani film and corroborates the incorporation of HSO_4^-/SO_4^{2-} within the polymer matrix. W was also detected in this zone, as Pani film was not thick enough to avoid the electron penetration to the substrate of PES-PPy/$PW_{12}O_{40}^{3-}$. However, a zonal analysis was performed in a zone where the substrate fibers could not be observed (Fig. 4-c). In the spectrum only S was observed, the film was thick enough to avoid the penetration of the electrons down to the substrate of PES-PPy/$PW_{12}O_{40}^{3-}$.

3.4. FTIR-ATR

Fig. 5 shows the spectrum for a sample of PES (a), PES-PPy/$PW_{12}O_{40}^{3-}$ (b), PES-PPy/$PW_{12}O_{40}^{3-}$ + Pani (21.6 C cm^{-2}) (c), and Pani powders (d). In the spectrum of polyester (Fig. 5-a) the different characteristic bands can be observed (the most representative are 723, 872, 960, 1014, 1090, 1236, 1338, 1408, 1505 and 1714 cm^{-1}). When polyester was covered with PPy/$PW_{12}O_{40}^{3-}$ different bands attributed to polypyrrole could be observed (Fig. 5-b). The most representative are: 781, 1040, 1128 and 1545 cm^{-1}, all of them described in our previous work [26]. The different bands of polyester are also present in the spectrum; since the layer of PPy/$PW_{12}O_{40}^{3-}$ is not thick enough to avoid the observation of the substrate bands (PES).

When Pani was electrochemically deposited on PES-PPy/$PW_{12}O_{40}^{3-}$ the spectrum was modified (21.6 C cm^{-2} of polymerization charge) (Fig. 5-c). To differentiate the Pani bands from the other contributions (PPy and PES), a spectrum of Pani powders obtained from the surface of the conducting fabric was also performed (Fig. 5-d).

The different contributions observed from the spectrum of the Pani powders were:

- Band located around 1550 cm^{-1}, C=C stretching in quinoid rings [47-50]

- Band located around 1450 cm^{-1}, C=C stretching in benzenoid rings [47-50].
- Band centered at 1300 cm^{-1}, C-N stretching in secondary amines probably related to leucoemeraldine [47,51].
- Band centered at 1200 cm^{-1}, C-N stretching [52].
- Bands around 1100, 1020, 900 and 800 cm^{-1}, attributed to C-H in-plane and out-of-plane bending of aniline rings [38].

The most representative band which appears in the spectrum of PES-PPy/$PW_{12}O_{40}^{3-}$ + Pani is located at 1300 cm^{-1} (C-N stretching in secondary amines) [47,51]. This band is not present in the PES (Fig. 5-a) and the PES-PPy/$PW_{12}O_{40}^{3-}$ spectrum (Fig. 5-b); so it is characteristic of polyaniline and its presence confirms the presence of polyaniline. The other bands that appear in the spectrum are overlapped with that of polypyrrole and polyester and make the assignment of the bands more complicated. When Pani is deposited on PES-PPy/$PW_{12}O_{40}^{3-}$, the greater thickness of the coating causes the diminution of the polyester bands. The PES bands are not clearly observed since its intensity has decreased.

3.5. Cyclic voltammetry measurements

Cyclic voltammetry measurements were performed for samples of PES-PPy/$PW_{12}O_{40}^{3-}$ and the samples of the same conducting fabric covered with Pani. Measurements were done in different pH solutions to test the electroactivity of the conducting fabrics in different media. The measurements were also made at different scan rates to see the influence of this parameter on the electrochemical response. To compare the electrochemical response, in all the figures it is shown the second scan obtained.

In Fig. 6-a it is shown the voltammograms obtained for the sample of PES-PPy/$PW_{12}O_{40}^{3-}$ in 0.5 M H_2SO_4 at the different scan rates (50, 5 and 1 mV s^{-1}). It can be seen that with the higher scan rate, no redox peaks were obtained and a resistive response was obtained. When the scan rate was lowered to 5 mV s^{-1}, the current density was lowered and a less resistive response was obtained. At 1 mV s^{-1}, the resistive response was not observed. The form of the voltammogram obtained was more similar to that obtained in bibliography since redox processes were observed [12]. As in Fig. 6-a, the different voltammograms have a common scale to compare the electrochemical response at the different scan rates, the form of the voltammogram cannot be clearly observed. In Fig. 6-b it can be observed better the voltammogram obtained for the lowest scan rate in 0.5 M H_2SO_4. Higher scan rates produce higher peak currents in the voltammograms. In our case, it is evident that the scan rate influences the electrochemical response of conducting fabrics obtained by cyclic voltammetry. Higher scan rates do not allow the observation of redox processes. On the other hand, lower scan rates permit the apparition of those processes. The explanation for these facts is that the substrate (polyester) is an insulating material; so the charge transference has to be produced along polypyrrole chains. The charge transfer begins from the zone below the electric contact and extends to the other parts of the electrode. If the scan rate is too fast (50 mV s^{-1}), there is not sufficient time to allow the transformation of the polymer and this is why a resistive response is obtained. When lower scan rates are employed, there is more time to allow the transformation of the polymer so the redox processes can be observed. This fact is clearly observed with the lowest scan rate (1 mV s^{-1}). Cyclic voltammetry studies of conducting polymers have been made on metallic substrates mainly; where the charge transfer is produced between the metal-polymer interface

instantaneously. Studies employing different scan rates have demonstrated that the form of the voltammogram is not changed by the scan rate; only the peak current of the redox processes is affected [53]. If insulating substrates are employed, the charge transfer is not produced instantaneously. Therefore, the scan rate in this case is an important parameter. As it will be explained later, the same behavior has been observed for the sample of conducting fabric covered with Pani. In Fig. 6-b it can be observed the voltammograms employing the lowest san rate (1 mV s^{-1}) in different pH solutions. The form of the voltammograms was similar in 0.5 M and 0.1 M H_2SO_4. In the pH 7 solution, the electroactivity of polypyrrole film was not substantially modified. In the pH 13 solution it was found a great lost of electroactivity; which is attributed to the deprotonation of polypyrrole that takes place at pH 10 [54]. During the formation of conducting polymers like polypyrrole or polyaniline, positive charges which are responsible for its electronic conduction (polarons and bipolarons) are created in its structure. These charges are compensated by counter ions to maintain the electroneutrality principle. The deprotonation of conducting polymers like polypyrrole and polyaniline causes the elimination of these positive charges. Conjugation breaking and release of doping anions are produced as a consequence [54]. When the deprotonation of conducting polymers occurs there is an excess of negative charge in the polymer, and the counter ion is expelled from the polymer matrix. That causes a substantial loss of conductivity in the conducting polymers. In the case of polypyrrole the loss of conductivity due to the deprotonation is about 3-4 orders of magnitude [54]. The $PW_{12}O_{40}^{3-}$ molecule also suffers a reaction of decomposition into PO_4^{3-} and WO_4^{2-} at pH>8.3 [55], contributing also to the loss of conductivity.

In Fig. 7-a it can be observed the voltammograms obtained for the sample of PES-PPy/$PW_{12}O_{40}^{3-}$ covered with Pani (10 C cm^{-2}). As in the case of the sample without Pani, it was observed a resistive response at 50 mV s^{-1}. When the scan rate was lowered the redox processes began to appear; at 1 mV s^{-1} it is noticeable the appearance of different redox peaks that can be observed better in Fig. 7-b or Fig. 8. The explanation for this fact is the same mentioned previously. It appears one oxidation peak at 0.47 V and a reduction one located at 0.26 V. A less resolved peak can also be observed at 0.42 V contained in the wider peak of 0.26 V. It can also be noticed that the current density is higher than in the case of the conducting fabric without Pani. The Pani deposit produces an increase of the material electroactivity due to the higher surface area of the globular deposit. For the sample containing only polypyrrole, an oxidation current density of about 0.1 mA cm^{-2} were reached at 0.4 V in 0.5 M H_2SO_4; when the Pani was deposited on the fabric (10 C cm^{-2}), approximately 1.5 mA cm^{-2} were obtained at 0.4 V. Fig. 7-b shows the voltammograms of PES-PPy/$PW_{12}O_{40}^{3-}$ + Pani (10 C cm^{-2}) in the different pH solutions. The voltammetric response in 0.5 M and 0.1 M H_2SO_4 was similar with similar current densities. However, in the case of the 0.1 M H_2SO_4 solution, the redox peaks were not clearly observed as in the case of 0.5 M H_2SO_4. Polyaniline protonation influences greatly the conductivity of Pani [56-58]. In the case of polyaniline, its deprotonation causes a loss of conductivity of about 9-10 orders of magnitude [56]. The contact with the pH 7 solution produced a decrease of the current density in the voltammogram. At pH 13 the decrease was greater than at pH 7. At these two last pHs, no redox peaks were observed due to polyaniline deprotonation.

Fig. 8 shows the comparison of the voltammograms obtained for samples covered with Pani with different polymerization charges (10 and 1.5 C cm^{-2}). It can be seen a clear

correlation between the current density (mA cm^{-2}) of the voltammograms with the polymerization charge (C cm^{-2}). The sample with the lowest polymerization charge showed peaks with lower current density, but the peaks observed were the same than the obtained for the sample with higher polymerization charge.

3.6. SECM measurements

Approach (I_T–L) curves were recorded in the feedback mode in a 0.01 M solution of $Ru(NH_3)_6^{3+}$ in 0.1 M KCl, pH ~5.2, using the 100-μm-diameter Pt tip held at a potential of -0.4 V vs Ag/AgCl (3 M KCl). According to the voltammogram in Fig. 9, this potential was selected to reduce the oxidized form of the mediator, $Ru(NH_3)_6^{3+}$, at a diffusion-controlled rate.

Approach curves give an indication of the electroactivity of the electrode surface. If the surface is non conductive, when the electrode approaches the surface there is a decrease of the current measured (negative feedback) [22]. On the other hand if the electrode is conductive, when the electrode approaches the surface of the substrate the current increases (positive feedback) [22].

Figure 10-a shows a selection of the experimental curves recorded at different points randomly chosen throughout the PES-PPy/$PW_{12}O_{40}^{3-}$ surface. The line scans of PES-PPy/$PW_{12}O_{40}^{3-}$ show different degrees of positive feedback. The positive feedback indicates an increase of the normalized current (I) when the microelectrode comes close to the surface, according to its conductive nature; ($I = i/i_\infty$ where $i_\infty = 4nFDaC$ in which n is the number of electrons involved in the reaction, F is the Faraday constant, D is the diffusion coefficient, a is the radius of the UME and C is the concentration of the reactant). On the other hand, for the sample containing only polyester (Fig. 10-a, dotted

line), negative feedback was obtained (I decreases with the normalized distance L = d/a in which d is the distance between UME and surface and a is the radius of the UME). Polyester is an insulating material and negative feedback was obtained. With this technique it is clearly shown the different electrochemical activity of the two surfaces analyzed.

In Fig. 10-b it is shown the electrochemical activity of PES-PPy/$PW_{12}O_{40}^{3-}$ + Pani substrate. The substrate containing Pani shows a bit less activity from L = 2 due to the fact that Pani is less conductive than polypyrrole at pH ~ 5.2. Polypyrrole is conductive in a wider pH range than polyaniline and maintains a good conductivity up to pH 10 [59]. The loss of conductivity after polypyrrole deprotonation is in the order of 3-4 orders of magnitude [54]. On the other hand, polyaniline conductivity is greatly affected by pH, at pH>4 suffers a great loss of electroactivity around 9-10 orders of magnitude [56]. The measurements were done in a solution with pH~5.2, so polyaniline was less conductive and that explains why the feedback obtained was less positive than the case of polypyrrole. However, the sample containing Pani continued acting as a conductor and not as an insulator (like polyester).

One main application of the SECM microscopy is the scanning of a surface to obtain 2D and 3D images of the electrochemical activity or topographical information [22]. In this work, the experiments were done at constant height, so the information of electroactivity and morphology cannot be discerned. The PES fabric topography presents significant differences (zones more elevated than others) and the polypyrrole coating obtained on the fabric was uniform, so topographical features of the fabric have more influence on the electrochemical response obtained than local differences of electroactivity. As example of this application, the 2D and 3D images of a PES-

PPy/$PW_{12}O_{40}^{3-}$ substrate are shown. In Fig. 11, it is shown the 2D and 3D images of a conductive PES-PPy/$PW_{12}O_{40}^{3-}$ substrate taken at constant height. In the 2D image, a SEM micrograph of the substrate surface has been superposed to illustrate the topographical influence on the response obtained. It is difficult to position the sample during the SECM analysis, which is why the micrograph is twisted. The more raised parts of the textile produce a higher increase of the current than the lower ones. The 3D image exemplifies better the influence of the textile topography on the electrochemical response obtained. The holes represent an increase of the current due to a major proximity of the substrate surface to the UME.

4. Conclusions

The electrochemical synthesis of Pani on conducting fabrics of PES-PPy/$PW_{12}O_{40}^{3-}$ has been achieved. XPS analyses have shown the formation of Pani with a higher doping level (N^+/N) than the original conducting fabric. Overoxidation was avoided at the synthesis potential of 1 V as C1s results showed. XPS and EDX analyses also showed the incorporation of S to the material, confirming the presence of sulphate/bisulphate anions as counter ions. FTIR-ATR showed the appearance of different bands attributed to Pani. The morphology of the Pani obtained by potentiostatic synthesis was globular, characteristic of films obtained by potentiostatic synthesis. Electrochemical characterization by CV showed the improvement of the electrical properties of the material when Pani was synthesized on the conducting fabrics. Moreover, the pH value and the scan rate were analyzed in the voltammetric response. Higher scan rates do not allow the observation of redox processes. Only lower scan rates produce the appearance

of these processes. This behavior could be explained by the fact that the substrate is an insulating material (polyester), so the charge transfer is produced across the conducting polymer. If high scan rates are employed, there is not sufficient time to allow the polymer transformation and then the electrochemical processes are not observed. In this work SECM measurements have been applied for the first time to study conducting fabrics properties. Approach curves showed negative feedback for plain polyester (insulating material) and positive feedback (conducting material) when polypyrrole was deposited on the surface of the fabric. Polyaniline deposit showed also positive feedback, although less positive than polypyrrole alone. This can be attributed to a loss of conductivity of polyaniline at the pH of measurement (~5.2). The pH range which allows conductive behavior of polypyrrole is higher than polyaniline one. Nevertheless, polyaniline coating maintains some degree of electroactivity. 2D and 3D images showed the influence of the morphological features of the fabric on the electrochemical response obtained. More work is in progress to evaluate the electroactivity of these electrodes in the degradation of organic molecules.

Acknowledgements

Authors thank to the Spanish Ministerio de Ciencia y Tecnología and European Union Funds (FEDER) (contract CTM2007-66570-C02-02 and CTM2010-18842-C02-02) and Universidad Politécnica de Valencia (Primeros Proyectos de Investigación (PAID-06-10)) for the financial support. J. Molina is grateful to the Conselleria d'Educació (Generalitat Valenciana) for the FPI fellowship. A.I. del Río is grateful to the Spanish Ministerio de Ciencia y Tecnología for the FPI fellowship.

References

[1] P. Lekpittaya, N. Yanumet, B.P. Grady, E.A. O'Rear, Resistivity of conductive polymer-coated fabric, J. Appl. Polym. Sci. 92 (2004) 2629-2636.

[2] D. Kincal, A. Kumar, A. Child, J. Reynolds, Conductivity switching in polypyrrole-coated textile fabrics as gas sensors, Synth. Met. 92 (1998) 53-56.

[3] J. Wu, D. Zhou, C.O. Too, G.G. Wallace, Conducting polymer coated lycra, Synth. Met. 155 (2005) 698-701.

[4] K.W. Oh, H.J. Park, S.H. Kim, Stretchable conductive fabric for electrotherapy, J. Appl. Polym. Sci. 88 (2003) 1225-1229.

[5] N.V. Bhat, D.T. Seshadri, M.N. Nate, A.V. Gore, Development of conductive cotton fabrics for heating devices, J. Appl. Polym. Sci. 102 (2006) 4690-4695.

[6] E. Hakansson, A. Kaynak, T. Lin, S. Nahavandi, T. Jones, E. Hu, Characterization of conducting polymer coated synthetic fabrics for heat generation, Synth. Met. 144 (2004) 21-28.

[7] J.P. Boutrois, R. Jolly, C. Pétrescu, Process of polypyrrole deposit on textile. Product characteristics and applications, Synth. Met. 85 (1997) 1405-1406.

[8] H. Kuhn, A. Child, W. Kimbrell, Toward real applications of conductive polymers, Synth. Met. 71 (1995) 2139-2142.

[9] R. Hirase, M. Hasegawa, M. Shirai, Conductive fibers based on poly(ethylene terephthalate)–polyaniline composites manufactured by electrochemical polymerization, J. Appl. Polym. Sci. 87 (2003) 1073-1078.

[10] S.N. Bhadani, M. Kumari, S.K. Sen Gupta, G.C. Sahu, Preparation of conducting fibers via the electrochemical polymerization of pyrrole, J. Appl. Polym. Sci. 64 (1997) 1073-1077.

[11] S.H. Kim, K.W. Oh, J.H. Bahk, Electrochemically synthesized polypyrrole and Cu-plated nylon/spandex for electrotherapeutic pad electrode, J. Appl. Polym. Sci. 91 (2004) 4064-4071.

[12] K.F. Babu, R. Senthilkumar, M. Noel, M.A. Kulandainathan, Polypyrrole microstructure deposited by chemical and electrochemical methods on cotton fabrics, Synth. Met. 159 (2009) 1353-1358.

[13] K. Bouzek, K.-M. Mangold, K. Jüttner, Electrocatalytic activity of platinum modified polypyrrole films for the methanol oxidation reaction, J. Appl. Electrochem. 31 (2001) 501-507.

[14] L. Li, Y. Zhang, J.-F. Drillet, R. Dittmeyer, K.-M. Jüttner, Preparation and characterization of Pt direct deposition on polypyrrole modified Nafion composite membranes for direct methanol fuel cell applications, Chem. Eng. J. 133 (2007) 113-119.

[15] F.J. Rodríguez, S. Gutiérrez, J.S. Ibanez, J.L. Bravo, N. Batina, The efficiency of toxic chromate reduction by a conducting polymer (polypyrrole): influence of electropolymerization conditions, Environ. Sci. Technol. 34 (2000) 2018-2023.

[16] Y. Tian, J. Wang, Z. Wang, S. Wang, Electroreduction of nitrite at an electrode modified with polypyrrole nanowires, Synth. Met. 143 (2004) 309-313.

[17] A. Lopes, S. Martins, A. Moraö, M. Magrinho, I. Gonçalves, Degradation of a textile dye C. I. Direct Red 80 by electrochemical processes, Port. Electrochim. Acta 22 (2004) 279-294.

[18] A.H. Gemeay, R.G. El-Sharkawy, I.A. Mansour, A.B. Zaki, Catalytic activity of polyaniline/MnO_2 composites towards the oxidative decolorization of organic dyes, Appl. Catal. B-Environ. 80 (2008) 106-115.

[19] A.H. Gemeay, R.G. El-Sharkawy, I.A. Mansour, A.B. Zaki, Preparation and characterization of polyaniline/manganese dioxide composites and their catalytic activity, J. Colloid Interf. Sci. 308 (2007) 385-394.

[20] H.S. Lee, J. Hong, Chemical synthesis and characterization of polypyrrole coated on porous membranes and its electrochemical stability, Synth. Met. 113 (2000) 115-119.

[21] J. Wu, D. Zhou, M.G. Looney, P.J. Waters, G.G. Wallace, C.O. Too., A molecular template approach to integration of polyaniline into textiles, Synth. Met. 159 (2009) 1135-1140.

[22] P. Sun, F.O. Laforge, M.V. Mirkin, Scanning electrochemical microscopy in the 21st century, Phys. Chem. Chem. Phys. 9 (2007) 802-823.

[23] M.V. Mirkin, B.R. Horrocks, Electroanalytical measurements using the scanning electrochemical microscope, Anal. Chim. Acta 406 (2000) 119-146.

[24] A.L. Barker, M. Gonsalves, J.V. Macpherson, C.J. Slevin, P.R. Unwin, Scanning electrochemical microscopy: beyond the solid/liquid interface, Anal. Chim. Acta 385 (1999) 223-240.

[25] Complete textile glossary. Available from: http://www.celaneseacetate.com/textile_glossary_filament_acetate.pdf; 2001 [accessed 15.5.10].

[26] J. Molina, A.I. del Río, J. Bonastre, F. Cases, Chemical and electrochemical polymerisation of pyrrole on polyester textiles in presence of phosphotungstic acid, Eur. Poly. J. 44 (2008) 2087-2098.

[27] J.M. Ribo, A. Dicko, J.M. Tura, D. Bloor, Chemical structure of polypyrrole: X-ray photoelectron spectroscopy of polypyrrole with 5-yliden-3-pyrrolin-2-one end groups, Polymer 32 (1991) 728-732.

[28] J.C. Thiéblemont, J.L. Gabelle, M.F. Planche, Polypyrrole overoxidation during its chemical synthesis, Synth. Met. 66 (1994) 243-247.

[29] M. Makhlouki, J.C. Bernède, M. Morsli, A. Bonnet, A. Conan, S. Lefrant, XPS study of conducting polypyrrole-poly(vinyl alcohol) composites, Synth. Met. 62 (1994) 101-106.

[30] R. Rajagopalan, J.O. Iroh, Characterization of polyaniline-polypyrrole composite coatingson low carbón steel: a XPS and infrared spectroscopy study, Appl. Surf. Sci. 218 (2003) 58-69.

[31] W. Prissanaroon-Ouajai, P.J. Pigram, R. Jones, A. Sirivat, A novel pH sensor based on hydroquinone monosulfonate-doped conducting polypyrrole, Sens. Actuators. B 135 (2008) 366-374.

[32] L.G. Paterno, S. Manolache, F. Denes, Synthesis of polyaniline-type thin layer structures under low-pressure RF-plasma conditions, Synth. Met. 130 (2002) 85-97.

[33] L. Sabbatini, C. Malitesta, E. De Giglio, I. Losito, L. Torsi, P.G. Zambonin, Electrosynthesised thin polymer films: the role of XPS in the design of application oriented innovative materials, J. Electron. Spectrosc. Relat. Phenom. 100 (1999) 35-53.

[34] J. Starck, P. Burg, S. Muller, J. Bimer, G. Furdin, P. Fioux, C.V. Guterl, D. Begin, P. Faure, B. Azambre, The influence of demineralisation and ammoxidation on the adsorption properties of an activated carbon prepared from a Polish lignite, Carbon 44 (2006) 2549-2557.

[35] C.G.J. Koopal, M.C. Feiters, R.J.M. Nolte, B. de Ruiter, R.B.M. Schasfoort, R. Czajka, H. Van Kempen, Polypyrrole microtubules and their use in the construction of a third generation biosensor, Synth. Met. 51 (1992) 397-405.

[36] L. Pesaresi, D.R. Brown, A.F. Lee, J.M. Montero, H. Williams, K. Wilson, Cs-doped $H_4SiW_{12}O_{40}$ catalysts for biodiesel applications, Appl. Catal. A 360 (2009) 50-58.

[37] M. Wahlqvist, A. Shchukarev, XPS spectra and electronic structure of Group IA sulfates, J. Electron. Spectrosc. Relat. Phenom. 156–158 (2007) 310-314.

[38] E.T. Kang, K.G. Neoh, K.L. Tan, Polyaniline: A polymer with many interesting intrinsic redox states, Prog. Polym. Sci. 23 (1998) 277-324.

[39] P. Pillay, D.E. Barnes, J.F. van Staden, Overcoming interference from hydrolysable cations during the determination of sulphuric acid by titration, Anal. Chim. Acta 440 (2001) 45-52.

[40] S. Carquigny, O. Segut, B. Lakard, F. Lallemand, P. Fievet, Effect of electrolyte solvent on the morphology of polypyrrole films: Application to the use of polypyrrole in pH sensors, Synth. Met. 158 (2008) 453-461.

[41] J. Mansouri, R.P. Burford, Characterization of PVDF-PPy composite membranes, Polymer 38 (1997) 6055-6069.

[42] A.P. Monkman, G.C. Stevens, D. Bloor, X-ray photoelectron spectroscopic investigations of the chain structure anddoping mechanisms in polyaniline, J. Phys. D. Appl. Phys. 24 (1991) 738-749.

[43] H. Schmiers, J. Friebel, P. Streubel, R. Hesse, R. Köpsel, Change of chemical bonding of nitrogen of polymeric N-heterocyclic compounds during pyrolysis, Carbon 37 (1999) 1965-1978.

[44] M.H. Pournaghi-Azar, B. Habibi, Electropolymerization of aniline in acid media on the bare and chemically pre-treated aluminum electrodes: A comparative characterization of the polyaniline deposited electrodes, Electrochim. Acta 52 (2007) 4222-4230.

[45] J. Desilvestro, W. Schelfele, Morphology of electrochemically prepared polyaniline. Influence of polymerization parameters, J. Mater. Chem. 3 (1993) 263-272.

[46] S.J. Choi, S.M. Park, Electrochemistry of conductive polymers. XXVI. Effects of electrolytes and growth methods on polyaniline morphology, J. Electrochem. Soc. 149 (2002) E26-E34.

[47] T. Osaka, Y. Ohnuki, N. Oyama, IR absorption spectroscopic identification of electroactive and electroinactive polyaniline films prepared by the electrochemical polymerization of aniline, J. Electroanal. Chem. 161 (1984) 399-406.

[48] J.-L. Camalet, J.-C. Lacroix, T.D. Nguyen, S. Aeiyach, M.C. Pham, J. Petitjean, P.-C. Lacaze, Aniline electropolymerization on platinum and mild steel from neutral aqueous media, J. Electroanal. Chem. 485 (2000) 13-20.

[49] R. Hirase, T. Shikata, M. Shirai, Selective formation of polyaniline on wool by chemical polymerization, using potassium iodate, Synth. Met. 146 (2004) 73-77.

[50] L. Wen, N.M. Kocherginsky, Doping-dependent ion selectivity of polyaniline membranes, Synth. Met. 106 (1999) 19-27.

[51] L. Jiang, Z. Cui, One-step synthesis of oriented polyaniline nanorods through electrochemical deposition, Polym. Bull. 56 (2006) 529-537.

[52] G. Socrates, Infrared Characteristic Group Frequencies (Tables and Charts), second ed., John Wiley & Sons, England, 1997.

[53] S.N. Bhadani, M.K. Gupta, S.K.S. Gupta, Cyclic voltammetry and conductivity investigations of polyaniline, J. Appl. Polym. Sci. 49 (1993) 397-403.

[54] M. Krzysztof, Chemical reactivity of polypyrrole and its relevance to polypyrrole based electrochemical sensors, Electroanal. 18 (2006) 1537-1551.

[55] Z. Zu, R. Tain, C. Rhodes, A study of the decomposition behaviour of 12-tungstophosphate heteropolyacid in solution, Can. J. Chem. 81 (2003) 1044-1050.

[56] A.G. MacDiarmid, Synthetic metals: a novel role for organic polymers, Synth. Met. 125 (2002) 11-22.

[57] F. Cases, F. Huerta, P. Garcés, E. Morallón, J.L. Vázquez, Voltammetric and in situ FTIRS study of the electrochemical oxidation of aniline from aqueous solutions buffered at pH 5, J. Electroanal. Chem. 501 (2001) 186-192.

[58] F. Cases, F. Huerta, R. Lapuente, C. Quijada, E. Morallón, J.L. Vázquez, Conducting films obtained by electro-oxidation of p-aminodiphenylamine (ADPA) in the presence of aniline in buffer aqueous solution at pH 5, J. Electroanal. Chem. 529 (2002) 59-65.

[59] H.N.T. Le, B. Garcia, C. Deslouis, Q.L. Xuan, Corrosion protection and conducting polymers: polypyrrole films on iron, Electrochim. Acta 46 (2001) 4259-4272.

Figure captions

Fig. 1. Potentiodynamic synthesis of Pani on conducting fabrics of PES-PPy/$PW_{12}O_{40}^{3-}$. Conditions: 0.5 M H_2SO_4, 0.5 M aniline, range potential: -0.2 V, +1.1 V, 5 mV s^{-1}, 5 scans.

Fig. 2. XPS high resolution spectra for C1s, O1s and N1s: PES-PPy/$PW_{12}O_{40}^{3-}$, (a) C1s, (c) O1s, (e) N1s; PES-PPy/$PW_{12}O_{40}^{3-}$ + Pani electrochemically synthesized (68 C cm^{-2}), (b) C1s, (d) O1s, (f) N1s.

Fig. 3. Micrographs of: (a) PES-PPy/$PW_{12}O_{40}^{3-}$; (b), (c), (d) PES-PPy/$PW_{12}O_{40}^{3-}$ + Pani (35 C cm^{-2}).

Fig. 4. EDX spectra of: (a) PES+PPy/$PW_{12}O_{40}^{3-}$, (b) and (c) PES+PPy//$PW_{12}O_{40}^{3-}$ + Pani (35 C cm^{-2}).

Fig. 5. FTIR-ATR spectrum of: (a) PES, (b) PES-PPy/$PW_{12}O_{40}^{3-}$, (c) PES-PPy/$PW_{12}O_{40}^{3-}$ + Pani (21.6 C cm^{-2}), (d) Pani powders.

Fig. 6. Cyclic voltammograms of PES-PPy/$PW_{12}O_{40}^{3-}$, second scan for all measurements: (a) 0.5 M H_2SO_4, 50, 5 and 1 mV s^{-1}, (b) 1 mV s^{-1}, pH 0, 0.7, 7 and 13.

Fig. 7. Cyclic voltammograms of PES-PPy/$PW_{12}O_{40}^{3-}$ + Pani (10 C cm^{-2}), second scan for all measurements: (a) 0.5 M H_2SO_4, 50, 5 and 1 mV s^{-1}, (b) 1 mV s^{-1}, pH 0, 0.7, 7 and 13.

Fig. 8. Cyclic voltammograms of PES-PPy/$PW_{12}O_{40}^{3-}$ + Pani, second scan for all measurements: 0.5 M H_2SO_4, comparison of 1.5 and 10 C cm^{-2} of polymerization charge.

Fig. 9. Cyclic voltammogram for Pt UME 100-μm-diameter tip. The UME potential was stepped from +100 to -700 mV (vs Ag/AgCl) in a 0.01 M $Ru(NH_3)_6^{3+}$ and 0.1 M KCl at 50 mV s^{-1}.

Fig. 10. Approaching curves for: (a) PES (---), PES-PPy/$PW_{12}O_{40}^{3-}$ (—) and (b) PES-PPy/$PW_{12}O_{40}^{3-}$ + PANI (1.5 C cm^{-2}) obtained with a 100 μm diameter Pt tip in 0.01 M $Ru(NH_3)_6^{3+}$ and 0.1 M KCl. The tip potential was -400 mV (vs Ag/AgCl) and the approach rate was 10 μm s^{-1}.

Fig. 11. 2D (SEM micrograph superposed) and 3D constant height SECM images of PES-PPy/$PW_{12}O_{40}^{3-}$, 0.25 cm^2 geometrical area. These images were taken with a 100 μm diameter Pt tip, in 0.01 M $Ru(NH_3)_6^{3+}$ and 0.1 M KCl at a constant height of 100 μm. The scan rate was 200 μm s^{-1} in comb mode; lengths of x and y lines were 1600 x 1400 μm with increments of 75 μm.

Table captions

Table 1. XPS surface compositional data for the samples analyzed.

Table 2. XPS results for binding energies (eV) for the samples analyzed.

Electrochemical synthesis of polyaniline on conducting fabrics of polyester covered with polypyrrole/$PW_{12}O_{40}^{3-}$. Chemical and electrochemical characterization.

J. Molina, J. Fernández, A.I. del Río, J. Bonastre, F. Cases *

Departamento de Ingeniería Textil y Papelera, EPS de Alcoy, Universidad Politécnica de Valencia, Plaza Ferrándiz y Carbonell s/n, 03801 Alcoy, Spain

Abstract

Polyaniline (Pani) has been electrochemically polymerized on conducting fabrics of polyester covered with polypyrrole/$PW_{12}O_{40}^{3-}$, obtaining a double conducting polymer layer. Electrochemical synthesis was performed by potentiostatic synthesis at 1 V. The chemical characterization of the material before and after Pani polymerization was performed by means of X-ray photoelectron spectroscopy (XPS), energy dispersive X-ray (EDX) and Fourier transform infrared spectroscopy (FTIR). The morphology of the coatings was observed employing scanning electron microscopy (SEM). The electrochemical characterization was performed by cyclic voltammetry (CV) and scanning electrochemical microscopy (SECM). It has been demonstrated that scan rate is an important parameter that influences the response obtained when characterizing conducting fabrics by CV. High scan rates do not allow the observation of redox peaks. However if lower scan rates are employed its apparition has been reported. The electrochemical deposit of polyaniline enhances the electroactivity of the material as it has been demonstrated by CV. SECM measurements showed local response with positive feedback (electroactive material) for the samples in open circuit conditions.

XPS analysis also showed a higher doping level (N^+/N), consistent with higher material electroactivity.

Keywords: Polyaniline, polypyrrole, conducting fabrics, cyclic voltammetry, SECM.

---

* Corresponding author. Fax.: +34 96 652 8438

E-mail address: fjcases@txp.upv.es (Prof. F. Cases)

1. Introduction

The production of textiles with new properties, such as conductivity, is a new field being investigated. The employment of conducting polymers is one of the methods that have been used to achieve this purpose. Polypyrrole (Ppy) has been the most employed conducting polymer when producing conducting fabrics [1-8]. The chemical polymerization of pyrrole in the presence of textile substrates produces a layer of conducting polymer on the fabrics. Applications of conducting polymers coated textiles are varied and numerous; like antistatic materials [1], gas sensors [2], biomechanical sensors [3], electrotherapy [4], heating devices [5-7] or microwave attenuation [8]. Another suitable method to produce conducting textiles is the electrochemical deposition of conducting polymers. The electrochemical polymerization is a more controlled method that only produces the conducting polymer on the surface of the desired electrode. The electrochemical polymerization can be performed indirectly or directly depending on the conductivity of the substrate employed as electrode. If the substrate is insulating, only an indirect electrochemical deposition can be performed.

Only few papers related to this topic can be seen in bibliography and the majority of them perform an indirect electrochemical deposition [9-12].

One of the applications that our group aims to is the employment of conducting fabrics in catalysis, or as a support with high surface area to electrodeposit Pt nanoparticles and enhance its electroactivity [13,14]. For instance, conducting polymers have been employed in environmental applications; electrodes modified with conducting polymers have been used in Cr^{6+} (toxic) reduction to Cr^{3+} (not toxic) [15] or nitrites electroreduction [16]. The employment of polypyrrole coated textiles in the electrochemical removal of the textile dye C. I. Direct Red 80 has also been reported [17]. Polyaniline/MnO_2 catalyst and H_2O_2 as an oxidant have been employed in the degradation of organic dyes such as Direct Red 81, Indigo Carmine and Acid Blue 92 [18,19].

In the present paper conducting textiles of polyester (PES) covered with polypyrrole/$PW_{12}O_{40}^{3-}$ have been produced to obtain a conducting substrate. Once the substrate was conductive, a direct electrochemical deposition of polyaniline was performed. In the end a double conducting polymer layer of polypyrrole/polyaniline was obtained. Chemical characterization of the conducting fabrics was done by XPS, EDX and FTIR-ATR; morphological characterization was done by means of SEM. The electrochemical and electrocatalytic properties of the monolayer and bilayer films have been measured by means of cyclic voltammetry (CV) and scanning electrochemical microscopy (SECM). In bibliography only a few assays of CV have been performed on conducting textiles [20,21]. In the present paper it is reported the influence of the scan rate in the characterization of conducting fabrics. The electroactivity of the samples was measured by scanning electrochemical microscopy (SECM). SECM is a relatively novel

(1989) and powerful technique that is becoming more popular among researchers [22-24]. Its employment in conducting fabrics has not been reported to our knowledge since the most employed substrate in bibliography is Pt.

2. Experimental

2.1. Reagents and materials

Analytical grade pyrrole, aniline, ferric chloride, sulphuric acid, sodium sulphate, sodium dihydrogenophosphate, disodium hydrogenophosphate and sodium hydroxide were provided by Merck. Normapur acetone was acquired from Prolabo. Analytical grade phosphotungstic acid hydrate was supplied by Fluka. Hexaammineruthenium (III) choride ($Ru(NH_3)_6Cl_3$) and potassium chloride were used as received from Acros Organics and Scharlau respectively. Solutions were deoxygenated by bubbling nitrogen (N_2 premier X50S). Ultrapure water was obtained from an Elix 3 Millipore-Milli-Q Advantage A10 system with a resistivity near to 18.2 MΩ cm.

Aniline was purified by distillation before use. Distillation was performed at reduced pressure in order to avoid thermal degradation of the monomer. After distillation aniline was stored in the dark at 0 ºC.

Polyester textile was acquired from Viatex S.A. and their characteristics were: fabric surface density, 140 g m^{-2}; warp threads per cm, 20 (warp linear density, 167 dtex); weft threads per cm, 60 (weft linear density, 500 dtex). These are specific terms used in the field of textile industry and their meaning can be consulted in a textile glossary [25].

2.2. Chemical synthesis of PPy/$PW_{12}O_{40}^{3-}$ on polyester fabrics

Chemical synthesis of PPy on polyester fabrics was done as reported in our previous study [26]. The size of the samples was 6 cm x 6 cm approximately. Previously to reaction, polyester was degreased with acetone in ultrasound bath and washed with water. Pyrrole concentration employed was 2 g l^{-1} and the molar relations of reagents employed in the chemical synthesis bath were pyrrole: $FeCl_3$: $H_3PW_{12}O_{40}$ (1: 2.5: 0.2). The next stage was the adsorption of pyrrole and counter ion ($PW_{12}O_{40}^{3-}$) (V=200 ml) on the fabric for 30 min in an ice bath without stirring. At the end of this time, the $FeCl_3$ solution (V=50 ml) was added and oxidation of the monomer took place during 150 min without stirring. Adsorption and reaction were performed in a precipitation beaker. The conducting fabric was washed with water to remove PPy not joined to fibers. The conducting fabric was dried in a desiccator for at least 24 h before measurements. The weight increase was measured obtaining a value around 10 %.

2.3. Electrochemical synthesis of Pani on conducting fabrics of PES-PPy/$PW_{12}O_{40}^{3-}$

Electrosynthesis of Pani on the fabrics of PES-PPy/$PW_{12}O_{40}^{3-}$ was performed using an Autolab PGSTAT302 potentiostat/galvanostat (Ecochemie). All electrochemical experiments were carried out at room temperature and without stirring. The counter electrodes (CE) were made of stainless steel. The working electrode (WE) was made cutting a strip of the conducting fabric (PES-PPy/$PW_{12}O_{40}^{3-}$) and locating it between two Titanium plates. Potential measurements were referred to Ag/AgCl (3 M KCl) reference electrode. Oxygen was removed from solution by bubbling nitrogen gas.

The conducting fabrics have an ohmic potential drop that needs to be compensated; otherwise the measured potentials will not be real. Therefore, the ohmic potential drop was measured and entered in the Autolab software.

The electrochemical synthesis of polyaniline was performed in 0.5 M H_2SO_4 and 0.5 M aniline aqueous solution, in N_2 atmosphere. The conducting fabric electrode was soaked with the solution to allow the diffusion of the monomer to the textile electrode. The method of synthesis employed was the potentiostatic synthesis. The synthesis potential for the potentiostatic synthesis was determined using cyclic voltammetry measurements; 1 V was selected as an adequate potential for the potentiostatic synthesis. For the potentiostatic synthesis, the potential was risen up from open circuit potential (ocp) of the electrode to 1 V. The electrosynthesis continued during the necessary time to achieve the desired electrical charge (C cm^{-2}).

2.4. FTIR-ATR spectroscopy

Fourier transform infrared spectroscopy with horizontal multirebound attenuated total reflection (FTIR-ATR) was performed with a Nicolet 6700 Spectrometer equipped with DTGS detector. An accessory with pressure control was employed to equalize the pressure in the different solid samples. A prism of ZnSe was employed. Spectra were collected with a resolution of 4 cm^{-1} and 100 scans were averaged for each sample.

2.5. X-Ray photoelectron spectroscopy

XPS analyses were conducted at a base pressure of at $5 \cdot 10^{-10}$ mbars and a temperature around 173 K. The XPS spectra were obtained with a VG-Microtech Multilab electron spectrometer by using unmonochromatized Mg K_α (1253.6 eV) radiation from a twin anode source operating at 300 W (20 mA, 15 KV). The binding energy (BE) scale was calibrated with reference to the C_{1s} line at 284.6 eV. The C1s, O1s and N1s core levels

spectra were analyzed for the sample of PES-PPy/$PW_{12}O_{40}^{3-}$ and the sample of PES-PPy/$PW_{12}O_{40}^{3-}$ + Pani.

2.6. SEM and EDX characterization

A Jeol JSM-6300 scanning electron microscope was employed to observe the morphology of the samples and perform EDX analyses. SEM analyses were performed using an acceleration voltage of 20 kV. EDX measurements were done between 0 and 20 keV.

2.7. Cyclic voltammetry measurements

An Autolab PGSTAT302 potentiostat/galvanostat was employed to perform CV measurements in the different pH solutions: pH~0 (0.5 M H_2SO_4), pH~0.7 (0.1 M H_2SO_4), pH~7 (NaH_2PO_4-NaH_2PO_4 buffer and Na_2SO_4 0.1 M), pH~13 (0.1 M NaOH and 0.1 M Na_2SO_4). Measurements were done at room temperature and without stirring. The CE employed was made of stainless steel; the pre-treatment consisted on polishing, degreasing with acetone in an ultrasonic bath and washing with water in the ultrasonic bath. The WE was made by cutting a strip of the conducting textile of PPy or the conducting textile of PPy covered with Pani. The sample was located between two Ti plates to perform the measurements. Potential measurements were referred to Ag/AgCl (3 M KCl) reference electrode. Oxygen was removed from solution by bubbling nitrogen gas for 10 min and then a N_2 atmosphere was maintained during the measurements. The ohmic potential drop was measured and introduced in the Autolab software. For the sample of PES-PPy/$PW_{12}O_{40}^{3-}$, the measurements were done between -0.4 V and +0.4 V. For the sample containing Pani, the potential range employed was -

0.2 V, +0.7 V. The characterization by means of CV has been done at different scan rates as it was corroborated the influence of this parameter on the electrochemical response obtained. The scan rates employed were 50 mV s^{-1}, 5 mV s^{-1} and 1 mV s^{-1}.

2.8. SECM measurements

SECM measurements were carried out with a scanning electrochemical microscope of Sensolytics. The three-electrode cell configuration consisted of a 100-μm-diameter Pt ultra-microelectrode (UME) working electrode, a Pt wire auxiliary electrode and an Ag/AgCl (3 M KCl) reference electrode. The solution selected for this study was 0.01 M $Ru(NH_3)_6Cl_3$ in aqueous 0.1 M KCl supporting electrolyte. All the experiments were carried out in inert nitrogen atmosphere. PES, PES-PPy/$PW_{12}O_{40}^{3-}$ and PES-PPy/$PW_{12}O_{40}^{3-}$ + Pani (1.5 C cm^{-2}) (0.25 cm^2 geometrical area) were chosen as substrates for the SECM measurements. The substrates were glued with epoxy resin on glass microscope slides.

The positioning of the Pt UME tip was achieved by first carefully putting it in contact with the substrate surface and then moving it in z direction (height of the electrode). Once the electrode was at the desired height, the electrode was approached to the substrate surface; the current of the UME was recorded to obtain the approach curves. Approach curves give us an indication of the electroactivity of the surface.

The surfaces were also scanned at their open circuit potential (OCP), and hence, the potential of the substrate was controlled indirectly by the redox couple concentration. Scanning the surface of the fabrics, a topographic profile of the sample was obtained.

3. Results and discussion

3.1. Electrochemical synthesis of Pani on PES-PPy/$PW_{12}O_{40}^{3-}$

The synthesis potential for the potentiostatic synthesis was established by cyclic voltammetry measurements (Fig. 1). The cyclic voltammetry measurements were carried out in the same conditions than the potentiostatic synthesis (0.5 M aniline and 0.5 M H_2SO_4). The potential was varied between -0.2 V and 1.1 V with a scan rate of 5 mV s^{-1}, 5 scans were registered. It can be seen that the current density grows with the number of scan, indicating that the Pani synthesis was being carried out. The potential of 1 V was selected as an adequate potential to carry out the potentiostatic synthesis because beyond this potential, the current density begin to grow sharply. As it will be explained later, at this potential overoxidation was not observed by means of XPS analyses.

3.2. XPS measurements

The C1s, O1s and N1s core levels spectra were analyzed for the sample of PES-PPy/$PW_{12}O_{40}^{3-}$ and the sample of PES-PPy/$PW_{12}O_{40}^{3-}$ covered with Pani. Table 1 shows chemical composition and doping ratio obtained by N analysis (N^+/N ratio) for both samples. The sample covered with Ppy/$PW_{12}O_{40}^{3-}$ should ideally have the formula $C_4H_3N(PW_{12}O_{40}^{3-})_x$, where "x" is the fractional doping level obtained by W analysis. XPS analysis showed a systematic carbon excess, which may be due to surface hydrocarbon contamination [27]. The composition analysis also showed an oxygen excess. This may be due to PPy ring oxidation attributed to PPy reaction with water as synthesis solvent [28]. The doping ratio obtained by nitrogen analysis, was in good agreement with the fractional doping level performed by tungsten analysis. The doping

ratio represented by the (N^+/N_{Total}) ratio was found to be 19.6%. As $PW_{12}O_{40}^{3-}$ presents 3 negative charges per molecule, the $PW_{12}O_{40}^{3-}$ fractional doping level would be 0.0196/3 = 0.065, close to 0.053 obtained by W analysis. For the sample covered with Pani/HSO_4^-/SO_4^{2-} there was a considerable difference between doping ratio estimated by atomic ratio N^+/N_{Total}, and doping level obtained by atomic ratio S/N. This discrepancy can be attributed to covalently bound sulfur bonds [29]. Covalently bound sulfur bonds belong to the polymeric structure, but they do not need positive charged nitrogen as polarons or bipolarons to accomplish the electroneutrality principle. So, the N^+ could be lower due to a minor number of polaronic sites. Table 2 shows the C1s, O1s, N1s core level binding energies assignments for the samples analyzed.

3.2.1. C1s analysis.

Fig. 2-a shows the deconvoluted high resolution C1s spectrum for the sample of PES-PPy/$PW_{12}O_{40}^{3-}$. Three peaks appear at the following binding energies: 284.1, 285.6 and 287.4 eV. The component at the lowest binding energy is due to C-C/C-H groups. The peak at 285.6 eV is assigned to C-N groups in the pyrrole rings [30-32]. The binding energy peak at 287.4 eV is ascribed to carbonyl C=O groups [33,34]. The appearance of C=O groups is mainly due to the presence of pyrrole overoxidation during chemical polymerization in aqueous media, as commented before. It has been proved that the polypyrrole is simultaneously degraded during the synthesis in short soluble maleimide molecules. This degradation process may be attributed to the polymer overoxidation which is described as a gradual polymer oxidation by water in the presence of $FeCl_3$. Quantitative measurements confirm that polymerization is second-order kinetics with respect to $FeCl_3$ while overoxidation appears to be only first order [28]. Contamination

with particulated PPy might also be on the surface due to the formation of aggregates and individual particles of colloidal PPy [35]. Fig. 2-a shows that C-C/C-H peak area is significantly greater than C-N one. For the pyrrole structure, the atomic ratio (C-C/C-H)/C-N must be equal to 1.0. The higher C-C/C-H contribution is coherent with a maleimide-like structure where C=O groups appears at α positions (C-N groups). This overoxidation might be roughly estimated as the atomic ratio $C{=}O/C_{Total}$, obtaining a value around 8 %. As surface hydrocarbon contamination may be present, this is a minimum value.

For the sample covered with Pani, Fig. 2-b shows two binding energy values for C1s core level at 284.2 and 285.8 eV. These contributions are related to C-C/C-H and C-N groups of the aniline ring, respectively. Peak corresponding to C=O group did not appear in the XPS analysis; so overoxidation was not present in the polyaniline layer. For this reason, the synthesis potential of 1 V was an adequate potential to perform the electrochemical synthesis as it was explained previously.

3.2.2. O1s analysis.

Fig. 2-c shows the high resolution O1s spectrum for the sample of PES-PPy/$PW_{12}O_{40}^{3-}$. The O1s core level peak was deconvoluted in two contributions centered at 530.3 and 531.7 eV. These contributions are assigned to W-O-W groups and W=O groups in the $PW_{12}O_{40}^{3-}$ counter ion respectively [36]. In Fig 2-d the high resolution O1s core level spectrum for the sample covered with Pani can be observed. The spectrum was deconvoluted in two peaks at 531.2 and 532.8 eV. These binding energies were assigned to SO_4^{2-} and HSO_4^- respectively [37], and are due to incorporated counter ion within the polymer. The proportion between HSO_4^-/SO_4^{2-} molecules was 1/3. Although

the low pH of the sulfuric synthesis solution might indicate a major amount of HSO_4^- as counterion, it is important to take into account that Pani is protonated in acid media [38], being able to displace the HSO_4^-/SO_4^{2-} equilibrium, pK_a=1.9 [39], to the formation of SO_4^{2-}.

3.2.3. N1s analysis.

Fig. 2-e shows the high resolution N1s spectrum for the sample of PES-PPy/$PW_{12}O_{40}^{3-}$. The N1s spectrum was deconvoluted into two contributions, centered at 399.7 and 401.9 eV. The peak at 399.7 eV was assigned to the neutral amine-like (–NH–) structure [30,33,40]. The peak at 401.9 eV was attributed to bipolaronic positively charged nitrogen, $=NH^+$ or N^{2+}. The electron-deficient nitrogen species arise from delocalization of electron density from the polypyrrole ring as a result of the formation of electronic defects (bipolarons) [31,40]. The doping ratio represented by the (N^{2+}/N_{Total}) ratio was found to be 19.6 %. Fig. 2-f shows the high resolution N1s spectrum for sample covered with Pani. The spectrum was deconvoluted in three peaks centered at 398.8, 399.7 and 401.6 eV. The first peak at 398.8 eV was attributed to deprotonated, uncharged, imine-like nitrogens (>C=N-) [30, 41-43]. The peak at 399.7 eV was assigned to the neutral amine-like (–NH–) structure. The peak at 401.6 eV was attributed to nitrogen atoms with a single positive charge, polaronic nitrogen N^+ [31]. The doping ratio (N^+/N_{Total}) was 22.4 %. The atomic ratios (>C=N-)/N_{Total} and (-NH)/N_{Total} were 31.5 and 46.1 %, respectively. The sum of atomic ratios for imine-like nitrogen and polaronic nitrogen was 53.9 %. This value is near to 50 % of an ideal intrinsically oxidized emeraldine structure [38]. These results confirm that conducting textiles covered with Pani were predominantly obtained in the emeraldine form. As it can be seen in Table 1, when the

electrochemical polymerization of polyaniline was performed, the doping ratio suffered a noticeable increase.

3.3. SEM and EDX measurements

In Fig. 3-a it can be seen the micrograph of the sample of PES-PPy/$PW_{12}O_{40}^{3-}$. As it can be observed, the whole fabric is covered by a layer of PPy/$PW_{12}O_{40}^{3-}$. The presence of polypyrrole aggregates is also noticeable. When the electrochemical synthesis of Pani was carried out, the entire surface of the fabric was covered by polyaniline. In Fig. 3-b it is shown a micrograph of the sample covered with Pani (35 C cm^{-2}) at low magnification (100x). The fibers of the fabric could hardly be observed as Pani had grown on the surface of the fibers and between the interstices of the fibers. In Fig. 3-c it is shown a zone where Pani was grown on the surface of the fibers. If Fig. 3-a and 3-c are compared, it can be observed the formation of a globular deposit on the surface of the fabric fibers. Micrograph in Fig. 3-d has been enhanced to observe better the deposit morphology. As it can be seen, Pani deposit presents a globular morphology. Similar morphology has been obtained when Pani was deposited by potentiostatic method on Al-Pt electrode [44]. The morphology of the Pani deposits depends on various factors, such as: polymerization conditions, synthesis technique, acid employed as electrolyte, etc [45,46].

EDX analyses were also performed to observe zonal composition in the samples analyzed. The EDX spectrum of the PES-PPy/$PW_{12}O_{40}^{3-}$ sample (Fig. 4-a) showed the presence of W, this indicates that the counter ion ($PW_{12}O_{40}^{3-}$) has been incorporated in the polypyrrole structure. The presence of Fe and Cl arise from the use of $FeCl_3$ as oxidant in polypyrrole synthesis. A zonal analysis was done on the surface of a fiber

covered with polyaniline (Fig. 4-b). The presence of S indicates the growth of the Pani film and corroborates the incorporation of HSO_4^-/SO_4^{2-} within the polymer matrix. W was also detected in this zone, as Pani film was not thick enough to avoid the electron penetration to the substrate of PES-PPy/$PW_{12}O_{40}^{3-}$. However, a zonal analysis was performed in a zone where the substrate fibers could not be observed (Fig. 4-c). In the spectrum only S was observed, the film was thick enough to avoid the penetration of the electrons down to the substrate of PES-PPy/$PW_{12}O_{40}^{3-}$.

3.4. FTIR-ATR

Fig. 5 shows the spectrum for a sample of PES (a), PES-PPy/$PW_{12}O_{40}^{3-}$ (b), PES-PPy/$PW_{12}O_{40}^{3-}$ + Pani (21.6 C cm^{-2}) (c), and Pani powders (d). In the spectrum of polyester (Fig. 5-a) the different characteristic bands can be observed (the most representative are 723, 872, 960, 1014, 1090, 1236, 1338, 1408, 1505 and 1714 cm^{-1}). When polyester was covered with PPy/$PW_{12}O_{40}^{3-}$ different bands attributed to polypyrrole could be observed (Fig. 5-b). The most representative are: 781, 1040, 1128 and 1545 cm^{-1}, all of them described in our previous work [26]. The different bands of polyester are also present in the spectrum; since the layer of PPy/$PW_{12}O_{40}^{3-}$ is not thick enough to avoid the observation of the substrate bands (PES).

When Pani was electrochemically deposited on PES-PPy/$PW_{12}O_{40}^{3-}$ the spectrum was modified (21.6 C cm^{-2} of polymerization charge) (Fig. 5-c). To differentiate the Pani bands from the other contributions (PPy and PES), a spectrum of Pani powders obtained from the surface of the conducting fabric was also performed (Fig. 5-d).

The different contributions observed from the spectrum of the Pani powders were:

- Band located around 1550 cm^{-1}, C=C stretching in quinoid rings [47-50]

- Band located around 1450 cm^{-1}, C=C stretching in benzenoid rings [47-50].
- Band centered at 1300 cm^{-1}, C-N stretching in secondary amines probably related to leucoemeraldine [47,51].
- Band centered at 1200 cm^{-1}, C-N stretching [52].
- Bands around 1100, 1020, 900 and 800 cm^{-1}, attributed to C-H in-plane and out-of-plane bending of aniline rings [38].

The most representative band which appears in the spectrum of PES-PPy/$PW_{12}O_{40}^{3-}$ + Pani is located at 1300 cm^{-1} (C-N stretching in secondary amines) [47,51]. This band is not present in the PES (Fig. 5-a) and the PES-PPy/$PW_{12}O_{40}^{3-}$ spectrum (Fig. 5-b); so it is characteristic of polyaniline and its presence confirms the presence of polyaniline. The other bands that appear in the spectrum are overlapped with that of polypyrrole and polyester and make the assignment of the bands more complicated. When Pani is deposited on PES-PPy/$PW_{12}O_{40}^{3-}$, the greater thickness of the coating causes the diminution of the polyester bands. The PES bands are not clearly observed since its intensity has decreased.

3.5. Cyclic voltammetry measurements

Cyclic voltammetry measurements were performed for samples of PES-PPy/$PW_{12}O_{40}^{3-}$ and the samples of the same conducting fabric covered with Pani. Measurements were done in different pH solutions to test the electroactivity of the conducting fabrics in different media. The measurements were also made at different scan rates to see the influence of this parameter on the electrochemical response. To compare the electrochemical response, in all the figures it is shown the second scan obtained.

In Fig. 6-a it is shown the voltammograms obtained for the sample of PES-PPy/$PW_{12}O_{40}^{3-}$ in 0.5 M H_2SO_4 at the different scan rates (50, 5 and 1 mV s^{-1}). It can be seen that with the higher scan rate, no redox peaks were obtained and a resistive response was obtained. When the scan rate was lowered to 5 mV s^{-1}, the current density was lowered and a less resistive response was obtained. At 1 mV s^{-1}, the resistive response was not observed. The form of the voltammogram obtained was more similar to that obtained in bibliography since redox processes were observed [12]. As in Fig. 6-a, the different voltammograms have a common scale to compare the electrochemical response at the different scan rates, the form of the voltammogram cannot be clearly observed. In Fig. 6-b it can be observed better the voltammogram obtained for the lowest scan rate in 0.5 M H_2SO_4. Higher scan rates produce higher peak currents in the voltammograms. In our case, it is evident that the scan rate influences the electrochemical response of conducting fabrics obtained by cyclic voltammetry. Higher scan rates do not allow the observation of redox processes. On the other hand, lower scan rates permit the apparition of those processes. The explanation for these facts is that the substrate (polyester) is an insulating material; so the charge transference has to be produced along polypyrrole chains. The charge transfer begins from the zone below the electric contact and extends to the other parts of the electrode. If the scan rate is too fast (50 mV s^{-1}), there is not sufficient time to allow the transformation of the polymer and this is why a resistive response is obtained. When lower scan rates are employed, there is more time to allow the transformation of the polymer so the redox processes can be observed. This fact is clearly observed with the lowest scan rate (1 mV s^{-1}). Cyclic voltammetry studies of conducting polymers have been made on metallic substrates mainly; where the charge transfer is produced between the metal-polymer interface

instantaneously. Studies employing different scan rates have demonstrated that the form of the voltammogram is not changed by the scan rate; only the peak current of the redox processes is affected [53]. If insulating substrates are employed, the charge transfer is not produced instantaneously. Therefore, the scan rate in this case is an important parameter. As it will be explained later, the same behavior has been observed for the sample of conducting fabric covered with Pani. In Fig. 6-b it can be observed the voltammograms employing the lowest san rate (1 mV s^{-1}) in different pH solutions. The form of the voltammograms was similar in 0.5 M and 0.1 M H_2SO_4. In the pH 7 solution, the electroactivity of polypyrrole film was not substantially modified. In the pH 13 solution it was found a great lost of electroactivity; which is attributed to the deprotonation of polypyrrole that takes place at pH 10 [54]. During the formation of conducting polymers like polypyrrole or polyaniline, positive charges which are responsible for its electronic conduction (polarons and bipolarons) are created in its structure. These charges are compensated by counter ions to maintain the electroneutrality principle. The deprotonation of conducting polymers like polypyrrole and polyaniline causes the elimination of these positive charges. Conjugation breaking and release of doping anions are produced as a consequence [54]. When the deprotonation of conducting polymers occurs there is an excess of negative charge in the polymer, and the counter ion is expelled from the polymer matrix. That causes a substantial loss of conductivity in the conducting polymers. In the case of polypyrrole the loss of conductivity due to the deprotonation is about 3-4 orders of magnitude [54]. The $PW_{12}O_{40}^{3-}$ molecule also suffers a reaction of decomposition into PO_4^{3-} and WO_4^{2-} at pH>8.3 [55], contributing also to the loss of conductivity.

In Fig. 7-a it can be observed the voltammograms obtained for the sample of PES-PPy/$PW_{12}O_{40}^{3-}$ covered with Pani (10 C cm^{-2}). As in the case of the sample without Pani, it was observed a resistive response at 50 mV s^{-1}. When the scan rate was lowered the redox processes began to appear; at 1 mV s^{-1} it is noticeable the appearance of different redox peaks that can be observed better in Fig. 7-b or Fig. 8. The explanation for this fact is the same mentioned previously. It appears one oxidation peak at 0.47 V and a reduction one located at 0.26 V. A less resolved peak can also be observed at 0.42 V contained in the wider peak of 0.26 V. It can also be noticed that the current density is higher than in the case of the conducting fabric without Pani. The Pani deposit produces an increase of the material electroactivity due to the higher surface area of the globular deposit. For the sample containing only polypyrrole, an oxidation current density of about 0.1 mA cm^{-2} were reached at 0.4 V in 0.5 M H_2SO_4; when the Pani was deposited on the fabric (10 C cm^{-2}), approximately 1.5 mA cm^{-2} were obtained at 0.4 V. Fig. 7-b shows the voltammograms of PES-PPy/$PW_{12}O_{40}^{3-}$ + Pani (10 C cm^{-2}) in the different pH solutions. The voltammetric response in 0.5 M and 0.1 M H_2SO_4 was similar with similar current densities. However, in the case of the 0.1 M H_2SO_4 solution, the redox peaks were not clearly observed as in the case of 0.5 M H_2SO_4. Polyaniline protonation influences greatly the conductivity of Pani [56-58]. In the case of polyaniline, its deprotonation causes a loss of conductivity of about 9-10 orders of magnitude [56]. The contact with the pH 7 solution produced a decrease of the current density in the voltammogram. At pH 13 the decrease was greater than at pH 7. At these two last pHs, no redox peaks were observed due to polyaniline deprotonation.

Fig. 8 shows the comparison of the voltammograms obtained for samples covered with Pani with different polymerization charges (10 and 1.5 C cm^{-2}). It can be seen a clear

correlation between the current density (mA cm^{-2}) of the voltammograms with the polymerization charge (C cm^{-2}). The sample with the lowest polymerization charge showed peaks with lower current density, but the peaks observed were the same than the obtained for the sample with higher polymerization charge.

3.6. SECM measurements

Approach (I_T–L) curves were recorded in the feedback mode in a 0.01 M solution of $Ru(NH_3)_6^{3+}$ in 0.1 M KCl, pH ~5.2, using the 100-μm-diameter Pt tip held at a potential of -0.4 V vs Ag/AgCl (3 M KCl). According to the voltammogram in Fig. 9, this potential was selected to reduce the oxidized form of the mediator, $Ru(NH_3)_6^{3+}$, at a diffusion-controlled rate.

Approach curves give an indication of the electroactivity of the electrode surface. If the surface is non conductive, when the electrode approaches the surface there is a decrease of the current measured (negative feedback) [22]. On the other hand if the electrode is conductive, when the electrode approaches the surface of the substrate the current increases (positive feedback) [22].

Figure 10-a shows a selection of the experimental curves recorded at different points randomly chosen throughout the PES-PPy/$PW_{12}O_{40}^{3-}$ surface. The line scans of PES-PPy/$PW_{12}O_{40}^{3-}$ show different degrees of positive feedback. The positive feedback indicates an increase of the normalized current (I) when the microelectrode comes close to the surface, according to its conductive nature; ($I = i/i_\infty$ where $i_\infty = 4nFDaC$ in which n is the number of electrons involved in the reaction, F is the Faraday constant, D is the diffusion coefficient, a is the radius of the UME and C is the concentration of the reactant). On the other hand, for the sample containing only polyester (Fig. 10-a, dotted

line), negative feedback was obtained (I decreases with the normalized distance L = d/a in which d is the distance between UME and surface and a is the radius of the UME). Polyester is an insulating material and negative feedback was obtained. With this technique it is clearly shown the different electrochemical activity of the two surfaces analyzed.

In Fig. 10-b it is shown the electrochemical activity of PES-PPy/$PW_{12}O_{40}^{3-}$ + Pani substrate. The substrate containing Pani shows a bit less activity from L = 2 due to the fact that Pani is less conductive than polypyrrole at pH ~ 5.2. Polypyrrole is conductive in a wider pH range than polyaniline and maintains a good conductivity up to pH 10 [59]. The loss of conductivity after polypyrrole deprotonation is in the order of 3-4 orders of magnitude [54]. On the other hand, polyaniline conductivity is greatly affected by pH, at pH>4 suffers a great loss of electroactivity around 9-10 orders of magnitude [56]. The measurements were done in a solution with pH~5.2, so polyaniline was less conductive and that explains why the feedback obtained was less positive than the case of polypyrrole. However, the sample containing Pani continued acting as a conductor and not as an insulator (like polyester).

One main application of the SECM microscopy is the scanning of a surface to obtain 2D and 3D images of the electrochemical activity or topographical information [22]. In this work, the experiments were done at constant height, so the information of electroactivity and morphology cannot be discerned. The PES fabric topography presents significant differences (zones more elevated than others) and the polypyrrole coating obtained on the fabric was uniform, so topographical features of the fabric have more influence on the electrochemical response obtained than local differences of electroactivity. As example of this application, the 2D and 3D images of a PES-

PPy/$PW_{12}O_{40}^{3-}$ substrate are shown. In Fig. 11, it is shown the 2D and 3D images of a conductive PES-PPy/$PW_{12}O_{40}^{3-}$ substrate taken at constant height. In the 2D image, a SEM micrograph of the substrate surface has been superposed to illustrate the topographical influence on the response obtained. It is difficult to position the sample during the SECM analysis, which is why the micrograph is twisted. The more raised parts of the textile produce a higher increase of the current than the lower ones. The 3D image exemplifies better the influence of the textile topography on the electrochemical response obtained. The holes represent an increase of the current due to a major proximity of the substrate surface to the UME.

4. Conclusions

The electrochemical synthesis of Pani on conducting fabrics of PES-PPy/$PW_{12}O_{40}^{3-}$ has been achieved. XPS analyses have shown the formation of Pani with a higher doping level (N^+/N) than the original conducting fabric. Overoxidation was avoided at the synthesis potential of 1 V as C1s results showed. XPS and EDX analyses also showed the incorporation of S to the material, confirming the presence of sulphate/bisulphate anions as counter ions. FTIR-ATR showed the appearance of different bands attributed to Pani. The morphology of the Pani obtained by potentiostatic synthesis was globular, characteristic of films obtained by potentiostatic synthesis. Electrochemical characterization by CV showed the improvement of the electrical properties of the material when Pani was synthesized on the conducting fabrics. Moreover, the pH value and the scan rate were analyzed in the voltammetric response. Higher scan rates do not allow the observation of redox processes. Only lower scan rates produce the appearance

of these processes. This behavior could be explained by the fact that the substrate is an insulating material (polyester), so the charge transfer is produced across the conducting polymer. If high scan rates are employed, there is not sufficient time to allow the polymer transformation and then the electrochemical processes are not observed. In this work SECM measurements have been applied for the first time to study conducting fabrics properties. Approach curves showed negative feedback for plain polyester (insulating material) and positive feedback (conducting material) when polypyrrole was deposited on the surface of the fabric. Polyaniline deposit showed also positive feedback, although less positive than polypyrrole alone. This can be attributed to a loss of conductivity of polyaniline at the pH of measurement (~5.2). The pH range which allows conductive behavior of polypyrrole is higher than polyaniline one. Nevertheless, polyaniline coating maintains some degree of electroactivity. 2D and 3D images showed the influence of the morphological features of the fabric on the electrochemical response obtained. More work is in progress to evaluate the electroactivity of these electrodes in the degradation of organic molecules.

Acknowledgements

Authors thank to the Spanish Ministerio de Ciencia y Tecnología and European Union Funds (FEDER) (contract CTM2007-66570-C02-02 and CTM2010-18842-C02-02) and Universidad Politécnica de Valencia (Primeros Proyectos de Investigación (PAID-06-10)) for the financial support. J. Molina is grateful to the Conselleria d'Educació (Generalitat Valenciana) for the FPI fellowship. A.I. del Río is grateful to the Spanish Ministerio de Ciencia y Tecnología for the FPI fellowship.

References

[1] P. Lekpittaya, N. Yanumet, B.P. Grady, E.A. O'Rear, Resistivity of conductive polymer-coated fabric, J. Appl. Polym. Sci. 92 (2004) 2629-2636.

[2] D. Kincal, A. Kumar, A. Child, J. Reynolds, Conductivity switching in polypyrrole-coated textile fabrics as gas sensors, Synth. Met. 92 (1998) 53-56.

[3] J. Wu, D. Zhou, C.O. Too, G.G. Wallace, Conducting polymer coated lycra, Synth. Met. 155 (2005) 698-701.

[4] K.W. Oh, H.J. Park, S.H. Kim, Stretchable conductive fabric for electrotherapy, J. Appl. Polym. Sci. 88 (2003) 1225-1229.

[5] N.V. Bhat, D.T. Seshadri, M.N. Nate, A.V. Gore, Development of conductive cotton fabrics for heating devices, J. Appl. Polym. Sci. 102 (2006) 4690-4695.

[6] E. Hakansson, A. Kaynak, T. Lin, S. Nahavandi, T. Jones, E. Hu, Characterization of conducting polymer coated synthetic fabrics for heat generation, Synth. Met. 144 (2004) 21-28.

[7] J.P. Boutrois, R. Jolly, C. Pétrescu, Process of polypyrrole deposit on textile. Product characteristics and applications, Synth. Met. 85 (1997) 1405-1406.

[8] H. Kuhn, A. Child, W. Kimbrell, Toward real applications of conductive polymers, Synth. Met. 71 (1995) 2139-2142.

[9] R. Hirase, M. Hasegawa, M. Shirai, Conductive fibers based on poly(ethylene terephthalate)–polyaniline composites manufactured by electrochemical polymerization, J. Appl. Polym. Sci. 87 (2003) 1073-1078.

[10] S.N. Bhadani, M. Kumari, S.K. Sen Gupta, G.C. Sahu, Preparation of conducting fibers via the electrochemical polymerization of pyrrole, J. Appl. Polym. Sci. 64 (1997) 1073-1077.

[11] S.H. Kim, K.W. Oh, J.H. Bahk, Electrochemically synthesized polypyrrole and Cu-plated nylon/spandex for electrotherapeutic pad electrode, J. Appl. Polym. Sci. 91 (2004) 4064-4071.

[12] K.F. Babu, R. Senthilkumar, M. Noel, M.A. Kulandainathan, Polypyrrole microstructure deposited by chemical and electrochemical methods on cotton fabrics, Synth. Met. 159 (2009) 1353-1358.

[13] K. Bouzek, K.-M. Mangold, K. Jüttner, Electrocatalytic activity of platinum modified polypyrrole films for the methanol oxidation reaction, J. Appl. Electrochem. 31 (2001) 501-507.

[14] L. Li, Y. Zhang, J.-F. Drillet, R. Dittmeyer, K.-M. Jüttner, Preparation and characterization of Pt direct deposition on polypyrrole modified Nafion composite membranes for direct methanol fuel cell applications, Chem. Eng. J. 133 (2007) 113-119.

[15] F.J. Rodríguez, S. Gutiérrez, J.S. Ibanez, J.L. Bravo, N. Batina, The efficiency of toxic chromate reduction by a conducting polymer (polypyrrole): influence of electropolymerization conditions, Environ. Sci. Technol. 34 (2000) 2018-2023.

[16] Y. Tian, J. Wang, Z. Wang, S. Wang, Electroreduction of nitrite at an electrode modified with polypyrrole nanowires, Synth. Met. 143 (2004) 309-313.

[17] A. Lopes, S. Martins, A. Moraö, M. Magrinho, I. Gonçalves, Degradation of a textile dye C. I. Direct Red 80 by electrochemical processes, Port. Electrochim. Acta 22 (2004) 279-294.

[18] A.H. Gemeay, R.G. El-Sharkawy, I.A. Mansour, A.B. Zaki, Catalytic activity of polyaniline/MnO_2 composites towards the oxidative decolorization of organic dyes, Appl. Catal. B-Environ. 80 (2008) 106-115.

[19] A.H. Gemeay, R.G. El-Sharkawy, I.A. Mansour, A.B. Zaki, Preparation and characterization of polyaniline/manganese dioxide composites and their catalytic activity, J. Colloid Interf. Sci. 308 (2007) 385-394.

[20] H.S. Lee, J. Hong, Chemical synthesis and characterization of polypyrrole coated on porous membranes and its electrochemical stability, Synth. Met. 113 (2000) 115-119.

[21] J. Wu, D. Zhou, M.G. Looney, P.J. Waters, G.G. Wallace, C.O. Too., A molecular template approach to integration of polyaniline into textiles, Synth. Met. 159 (2009) 1135-1140.

[22] P. Sun, F.O. Laforge, M.V. Mirkin, Scanning electrochemical microscopy in the 21st century, Phys. Chem. Chem. Phys. 9 (2007) 802-823.

[23] M.V. Mirkin, B.R. Horrocks, Electroanalytical measurements using the scanning electrochemical microscope, Anal. Chim. Acta 406 (2000) 119-146.

[24] A.L. Barker, M. Gonsalves, J.V. Macpherson, C.J. Slevin, P.R. Unwin, Scanning electrochemical microscopy: beyond the solid/liquid interface, Anal. Chim. Acta 385 (1999) 223-240.

[25] Complete textile glossary. Available from: http://www.celaneseacetate.com/textile_glossary_filament_acetate.pdf; 2001 [accessed 15.5.10].

[26] J. Molina, A.I. del Río, J. Bonastre, F. Cases, Chemical and electrochemical polymerisation of pyrrole on polyester textiles in presence of phosphotungstic acid, Eur. Poly. J. 44 (2008) 2087-2098.

[27] J.M. Ribo, A. Dicko, J.M. Tura, D. Bloor, Chemical structure of polypyrrole: X-ray photoelectron spectroscopy of polypyrrole with 5-yliden-3-pyrrolin-2-one end groups, Polymer 32 (1991) 728-732.

[28] J.C. Thiéblemont, J.L. Gabelle, M.F. Planche, Polypyrrole overoxidation during its chemical synthesis, Synth. Met. 66 (1994) 243-247.

[29] M. Makhlouki, J.C. Bernède, M. Morsli, A. Bonnet, A. Conan, S. Lefrant, XPS study of conducting polypyrrole-poly(vinyl alcohol) composites, Synth. Met. 62 (1994) 101-106.

[30] R. Rajagopalan, J.O. Iroh, Characterization of polyaniline-polypyrrole composite coatingson low carbón steel: a XPS and infrared spectroscopy study, Appl. Surf. Sci. 218 (2003) 58-69.

[31] W. Prissanaroon-Ouajai, P.J. Pigram, R. Jones, A. Sirivat, A novel pH sensor based on hydroquinone monosulfonate-doped conducting polypyrrole, Sens. Actuators. B 135 (2008) 366-374.

[32] L.G. Paterno, S. Manolache, F. Denes, Synthesis of polyaniline-type thin layer structures under low-pressure RF-plasma conditions, Synth. Met. 130 (2002) 85-97.

[33] L. Sabbatini, C. Malitesta, E. De Giglio, I. Losito, L. Torsi, P.G. Zambonin, Electrosynthesised thin polymer films: the role of XPS in the design of application oriented innovative materials, J. Electron. Spectrosc. Relat. Phenom. 100 (1999) 35-53.

[34] J. Starck, P. Burg, S. Muller, J. Bimer, G. Furdin, P. Fioux, C.V. Guterl, D. Begin, P. Faure, B. Azambre, The influence of demineralisation and ammoxidation on the adsorption properties of an activated carbon prepared from a Polish lignite, Carbon 44 (2006) 2549-2557.

[35] C.G.J. Koopal, M.C. Feiters, R.J.M. Nolte, B. de Ruiter, R.B.M. Schasfoort, R. Czajka, H. Van Kempen, Polypyrrole microtubules and their use in the construction of a third generation biosensor, Synth. Met. 51 (1992) 397-405.

[36] L. Pesaresi, D.R. Brown, A.F. Lee, J.M. Montero, H. Williams, K. Wilson, Cs-doped $H_4SiW_{12}O_{40}$ catalysts for biodiesel applications, Appl. Catal. A 360 (2009) 50-58.

[37] M. Wahlqvist, A. Shchukarev, XPS spectra and electronic structure of Group IA sulfates, J. Electron. Spectrosc. Relat. Phenom. 156–158 (2007) 310-314.

[38] E.T. Kang, K.G. Neoh, K.L. Tan, Polyaniline: A polymer with many interesting intrinsic redox states, Prog. Polym. Sci. 23 (1998) 277-324.

[39] P. Pillay, D.E. Barnes, J.F. van Staden, Overcoming interference from hydrolysable cations during the determination of sulphuric acid by titration, Anal. Chim. Acta 440 (2001) 45-52.

[40] S. Carquigny, O. Segut, B. Lakard, F. Lallemand, P. Fievet, Effect of electrolyte solvent on the morphology of polypyrrole films: Application to the use of polypyrrole in pH sensors, Synth. Met. 158 (2008) 453-461.

[41] J. Mansouri, R.P. Burford, Characterization of PVDF-PPy composite membranes, Polymer 38 (1997) 6055-6069.

[42] A.P. Monkman, G.C. Stevens, D. Bloor, X-ray photoelectron spectroscopic investigations of the chain structure anddoping mechanisms in polyaniline, J. Phys. D. Appl. Phys. 24 (1991) 738-749.

[43] H. Schmiers, J. Friebel, P. Streubel, R. Hesse, R. Köpsel, Change of chemical bonding of nitrogen of polymeric N-heterocyclic compounds during pyrolysis, Carbon 37 (1999) 1965-1978.

[44] M.H. Pournaghi-Azar, B. Habibi, Electropolymerization of aniline in acid media on the bare and chemically pre-treated aluminum electrodes: A comparative characterization of the polyaniline deposited electrodes, Electrochim. Acta 52 (2007) 4222-4230.

[45] J. Desilvestro, W. Schelfele, Morphology of electrochemically prepared polyaniline. Influence of polymerization parameters, J. Mater. Chem. 3 (1993) 263-272.

[46] S.J. Choi, S.M. Park, Electrochemistry of conductive polymers. XXVI. Effects of electrolytes and growth methods on polyaniline morphology, J. Electrochem. Soc. 149 (2002) E26-E34.

[47] T. Osaka, Y. Ohnuki, N. Oyama, IR absorption spectroscopic identification of electroactive and electroinactive polyaniline films prepared by the electrochemical polymerization of aniline, J. Electroanal. Chem. 161 (1984) 399-406.

[48] J.-L. Camalet, J.-C. Lacroix, T.D. Nguyen, S. Aeiyach, M.C. Pham, J. Petitjean, P.-C. Lacaze, Aniline electropolymerization on platinum and mild steel from neutral aqueous media, J. Electroanal. Chem. 485 (2000) 13-20.

[49] R. Hirase, T. Shikata, M. Shirai, Selective formation of polyaniline on wool by chemical polymerization, using potassium iodate, Synth. Met. 146 (2004) 73-77.

[50] L. Wen, N.M. Kocherginsky, Doping-dependent ion selectivity of polyaniline membranes, Synth. Met. 106 (1999) 19-27.

[51] L. Jiang, Z. Cui, One-step synthesis of oriented polyaniline nanorods through electrochemical deposition, Polym. Bull. 56 (2006) 529-537.

[52] G. Socrates, Infrared Characteristic Group Frequencies (Tables and Charts), second ed., John Wiley & Sons, England, 1997.

[53] S.N. Bhadani, M.K. Gupta, S.K.S. Gupta, Cyclic voltammetry and conductivity investigations of polyaniline, J. Appl. Polym. Sci. 49 (1993) 397-403.

[54] M. Krzysztof, Chemical reactivity of polypyrrole and its relevance to polypyrrole based electrochemical sensors, Electroanal. 18 (2006) 1537-1551.

[55] Z. Zu, R. Tain, C. Rhodes, A study of the decomposition behaviour of 12-tungstophosphate heteropolyacid in solution, Can. J. Chem. 81 (2003) 1044-1050.

[56] A.G. MacDiarmid, Synthetic metals: a novel role for organic polymers, Synth. Met. 125 (2002) 11-22.

[57] F. Cases, F. Huerta, P. Garcés, E. Morallón, J.L. Vázquez, Voltammetric and in situ FTIRS study of the electrochemical oxidation of aniline from aqueous solutions buffered at pH 5, J. Electroanal. Chem. 501 (2001) 186-192.

[58] F. Cases, F. Huerta, R. Lapuente, C. Quijada, E. Morallón, J.L. Vázquez, Conducting films obtained by electro-oxidation of p-aminodiphenylamine (ADPA) in the presence of aniline in buffer aqueous solution at pH 5, J. Electroanal. Chem. 529 (2002) 59-65.

[59] H.N.T. Le, B. Garcia, C. Deslouis, Q.L. Xuan, Corrosion protection and conducting polymers: polypyrrole films on iron, Electrochim. Acta 46 (2001) 4259-4272.

Figure captions

Fig. 1. Potentiodynamic synthesis of Pani on conducting fabrics of PES-PPy/$PW_{12}O_{40}^{3-}$. Conditions: 0.5 M H_2SO_4, 0.5 M aniline, range potential: -0.2 V, +1.1 V, 5 mV s^{-1}, 5 scans.

Fig. 2. XPS high resolution spectra for C1s, O1s and N1s: PES-PPy/$PW_{12}O_{40}^{3-}$, (a) C1s, (c) O1s, (e) N1s; PES-PPy/$PW_{12}O_{40}^{3-}$ + Pani electrochemically synthesized (68 C cm^{-2}), (b) C1s, (d) O1s, (f) N1s.

Fig. 3. Micrographs of: (a) PES-PPy/$PW_{12}O_{40}^{3-}$; (b), (c), (d) PES-PPy/$PW_{12}O_{40}^{3-}$ + Pani (35 C cm^{-2}).

Fig. 4. EDX spectra of: (a) PES+PPy/$PW_{12}O_{40}^{3-}$, (b) and (c) PES+PPy//$PW_{12}O_{40}^{3-}$ + Pani (35 C cm^{-2}).

Fig. 5. FTIR-ATR spectrum of: (a) PES, (b) PES-PPy/$PW_{12}O_{40}^{3-}$, (c) PES-PPy/$PW_{12}O_{40}^{3-}$ + Pani (21.6 C cm^{-2}), (d) Pani powders.

Fig. 6. Cyclic voltammograms of PES-PPy/$PW_{12}O_{40}^{3-}$, second scan for all measurements: (a) 0.5 M H_2SO_4, 50, 5 and 1 mV s^{-1}, (b) 1 mV s^{-1}, pH 0, 0.7, 7 and 13.

Fig. 7. Cyclic voltammograms of PES-PPy/$PW_{12}O_{40}^{3-}$ + Pani (10 C cm^{-2}), second scan for all measurements: (a) 0.5 M H_2SO_4, 50, 5 and 1 mV s^{-1}, (b) 1 mV s^{-1}, pH 0, 0.7, 7 and 13.

Fig. 8. Cyclic voltammograms of PES-PPy/$PW_{12}O_{40}^{3-}$ + Pani, second scan for all measurements: 0.5 M H_2SO_4, comparison of 1.5 and 10 C cm^{-2} of polymerization charge.

Fig. 9. Cyclic voltammogram for Pt UME 100-μm-diameter tip. The UME potential was stepped from +100 to -700 mV (vs Ag/AgCl) in a 0.01 M $Ru(NH_3)_6^{3+}$ and 0.1 M KCl at 50 mV s^{-1}.

Fig. 10. Approaching curves for: (a) PES (---), PES-PPy/$PW_{12}O_{40}^{3-}$ (—) and (b) PES-PPy/$PW_{12}O_{40}^{3-}$ + PANI (1.5 C cm^{-2}) obtained with a 100 μm diameter Pt tip in 0.01 M $Ru(NH_3)_6^{3+}$ and 0.1 M KCl. The tip potential was -400 mV (vs Ag/AgCl) and the approach rate was 10 μm s^{-1}.

Fig. 11. 2D (SEM micrograph superposed) and 3D constant height SECM images of PES-PPy/$PW_{12}O_{40}^{3-}$, 0.25 cm^2 geometrical area. These images were taken with a 100 μm diameter Pt tip, in 0.01 M $Ru(NH_3)_6^{3+}$ and 0.1 M KCl at a constant height of 100 μm. The scan rate was 200 μm s^{-1} in comb mode; lengths of x and y lines were 1600 x 1400 μm with increments of 75 μm.

Table captions

Table 1. XPS surface compositional data for the samples analyzed.

Table 2. XPS results for binding energies (eV) for the samples analyzed.

Figure 1

Click here to download high resolution image

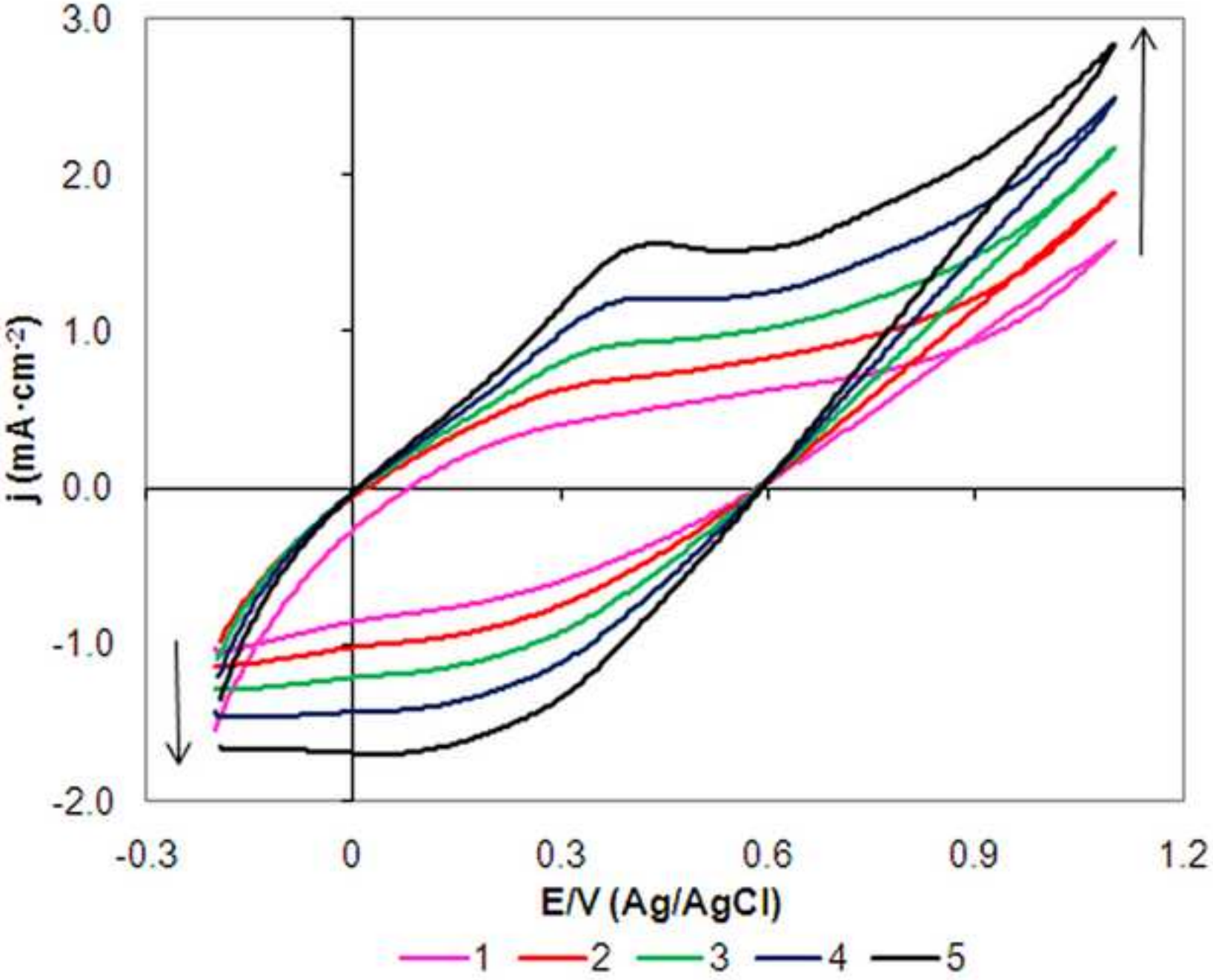

Figure 2

Click here to download high resolution image

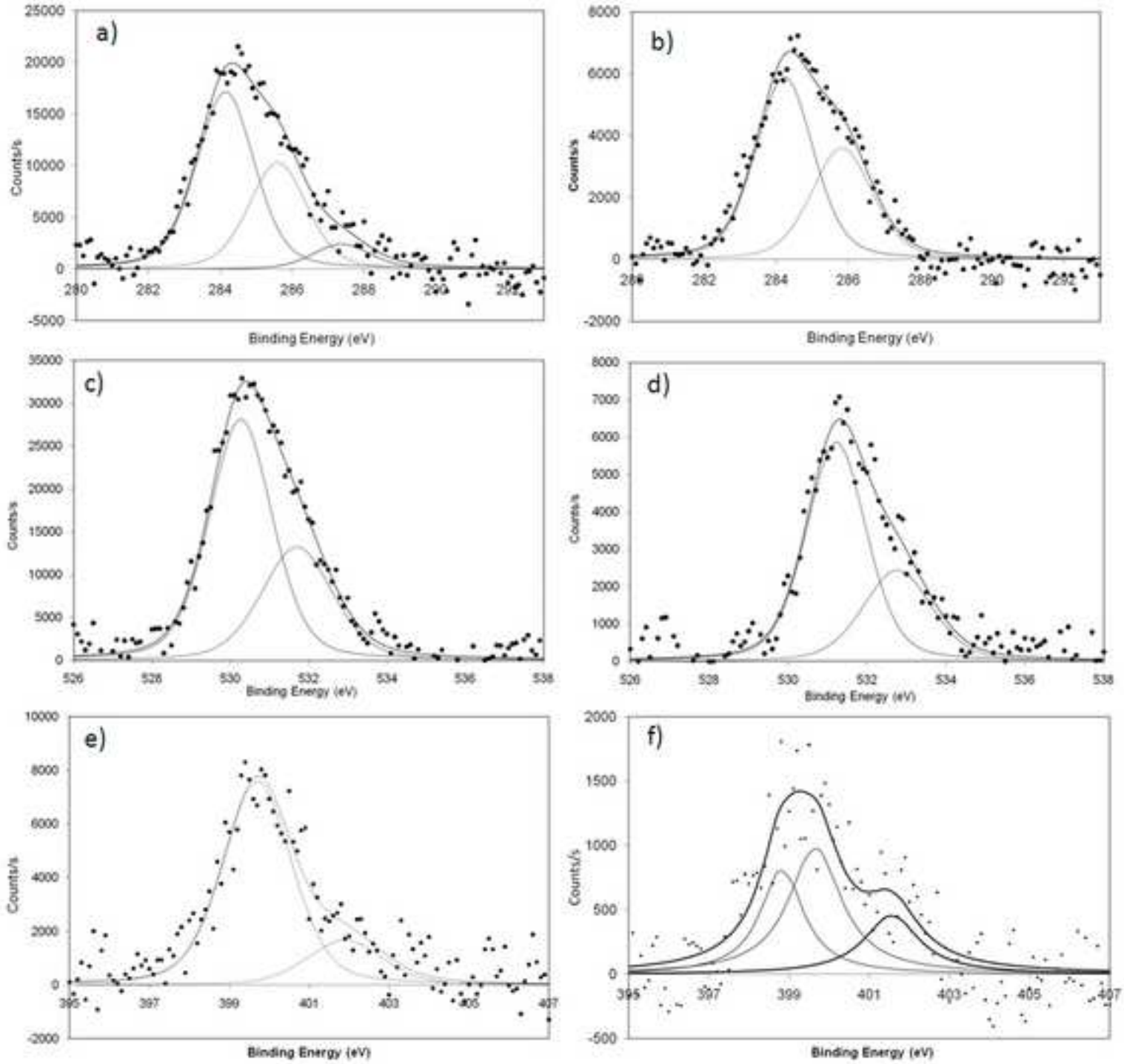

Figure 3

Click here to download high resolution image

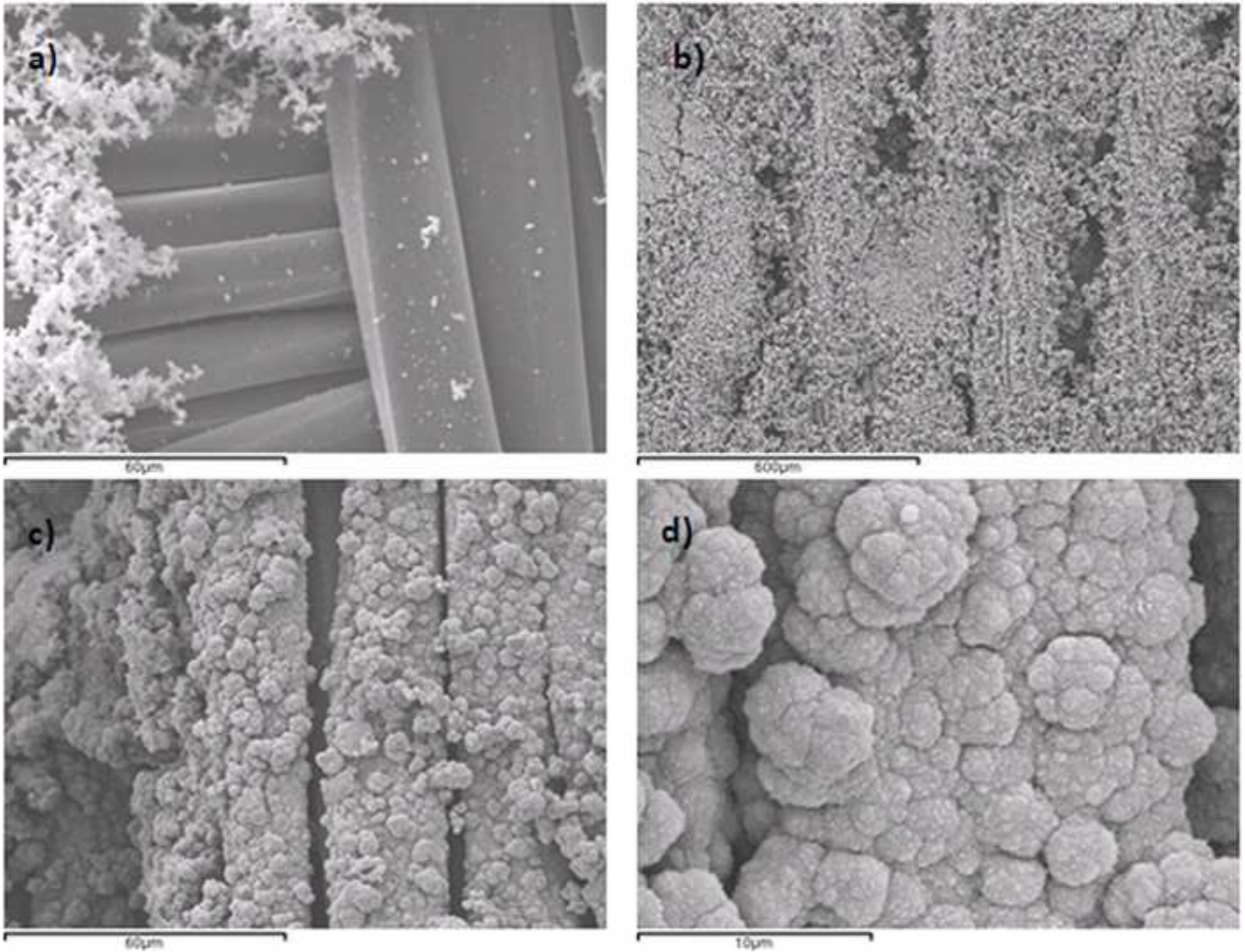

Figure 4

Click here to download high resolution image

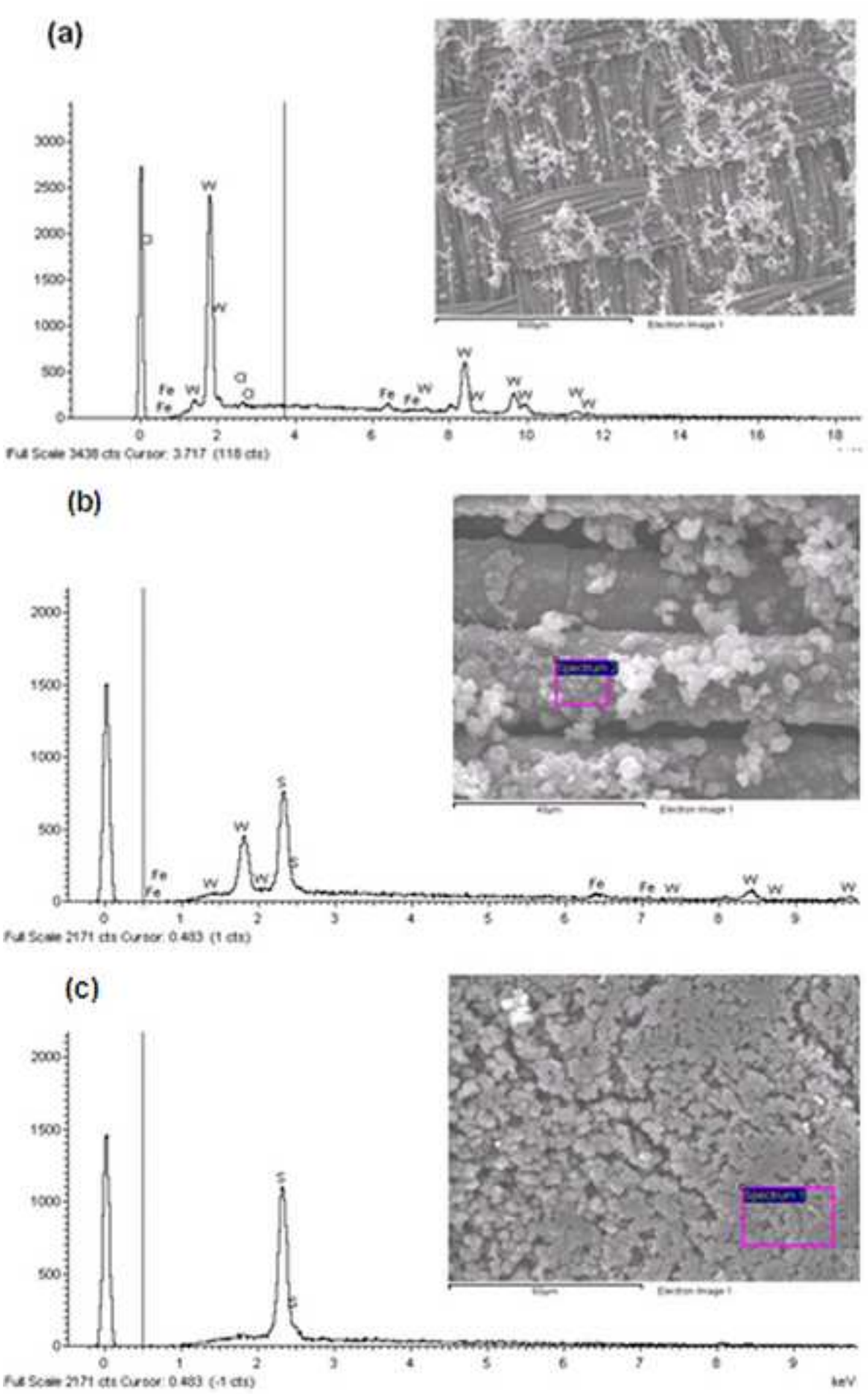

Figure 5

Click here to download high resolution image

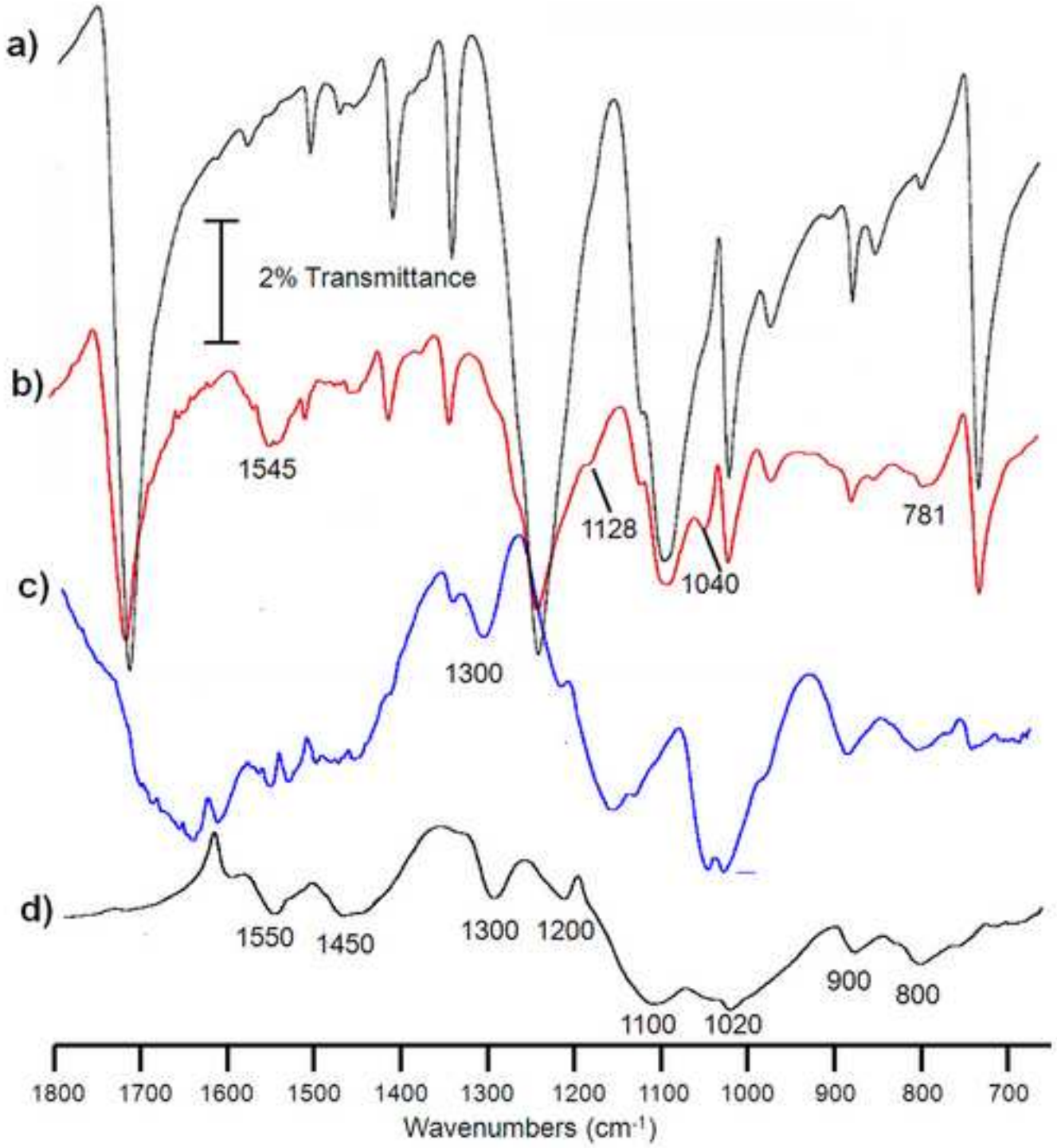

Figure 6

Click here to download high resolution image

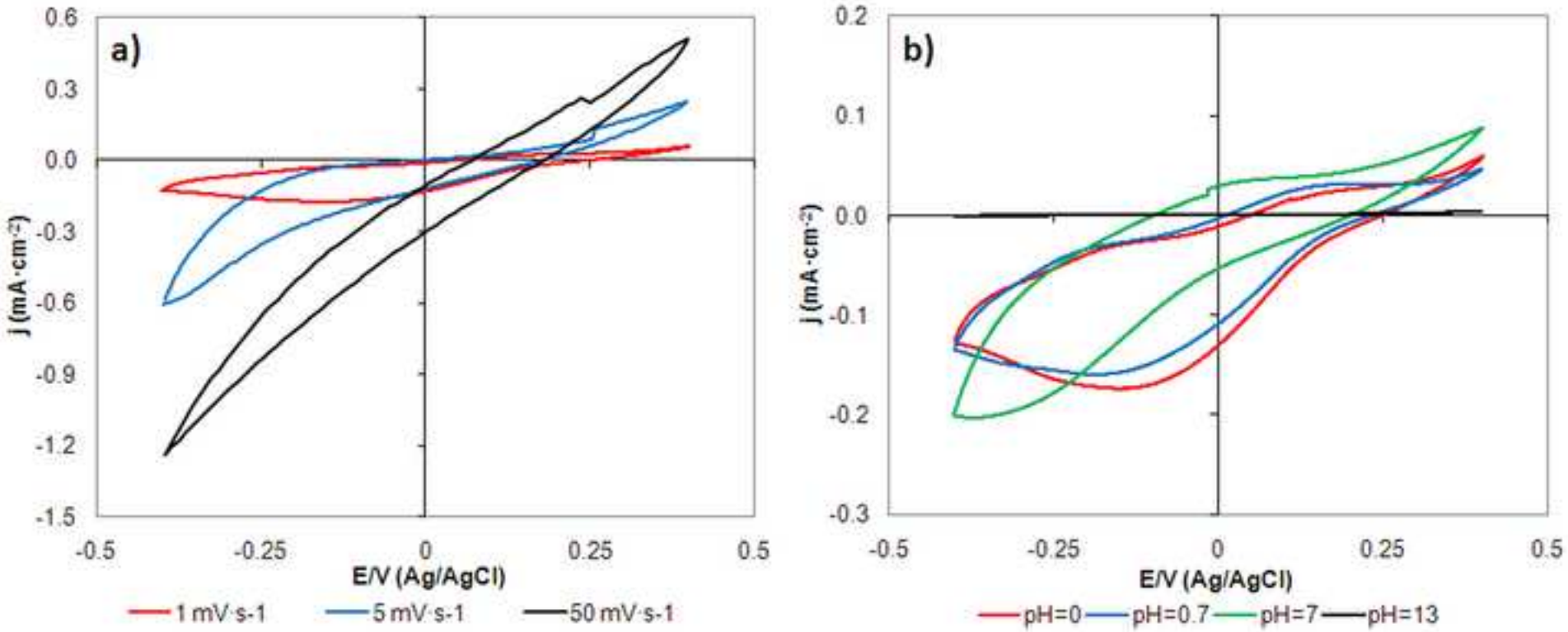

Figure 7

Click here to download high resolution image

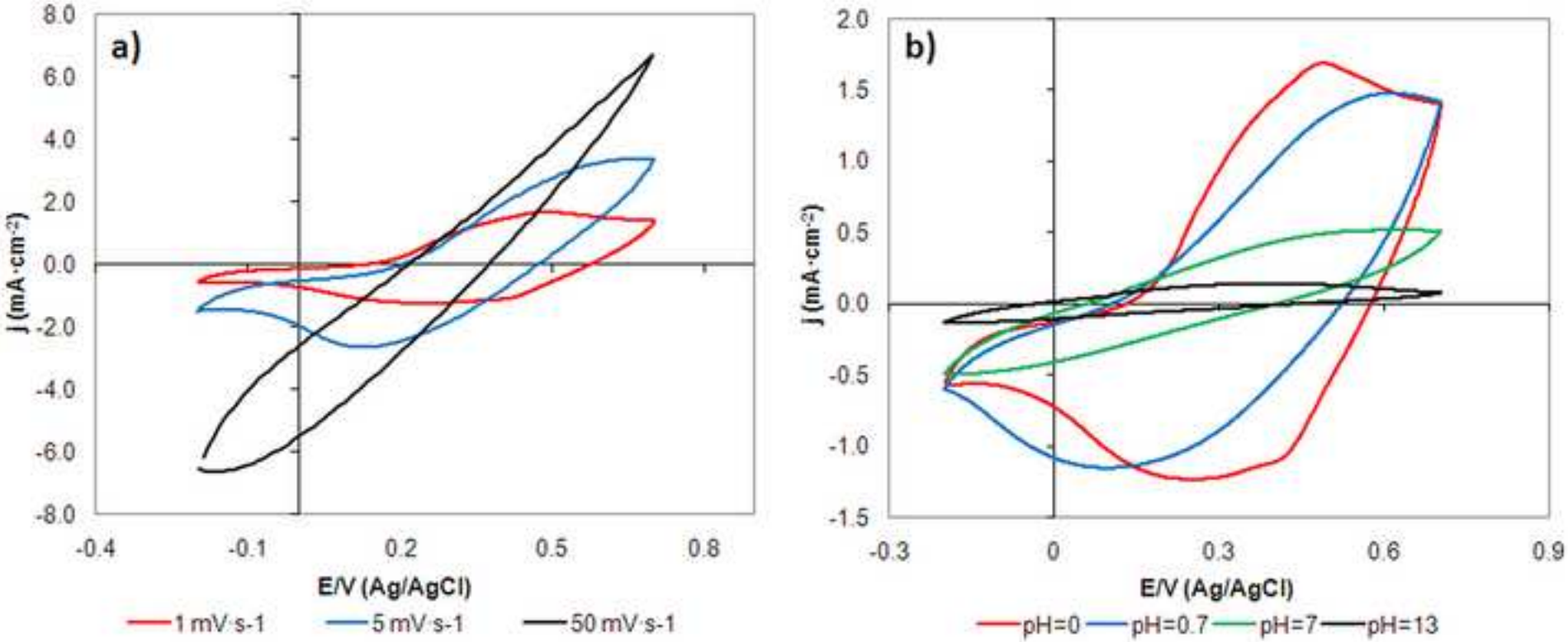

Figure 8

Click here to download high resolution image

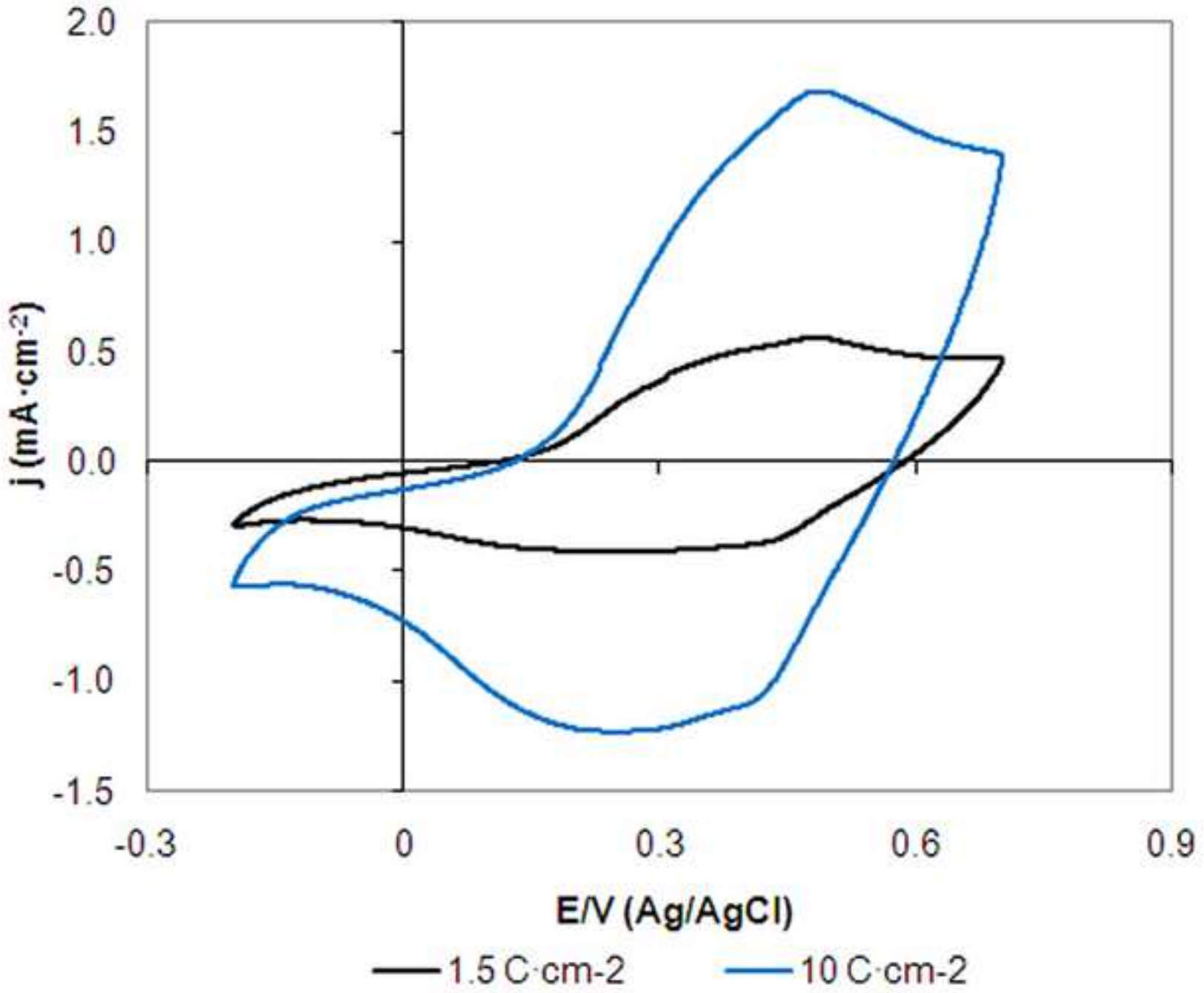

Figure 9

Click here to download high resolution image

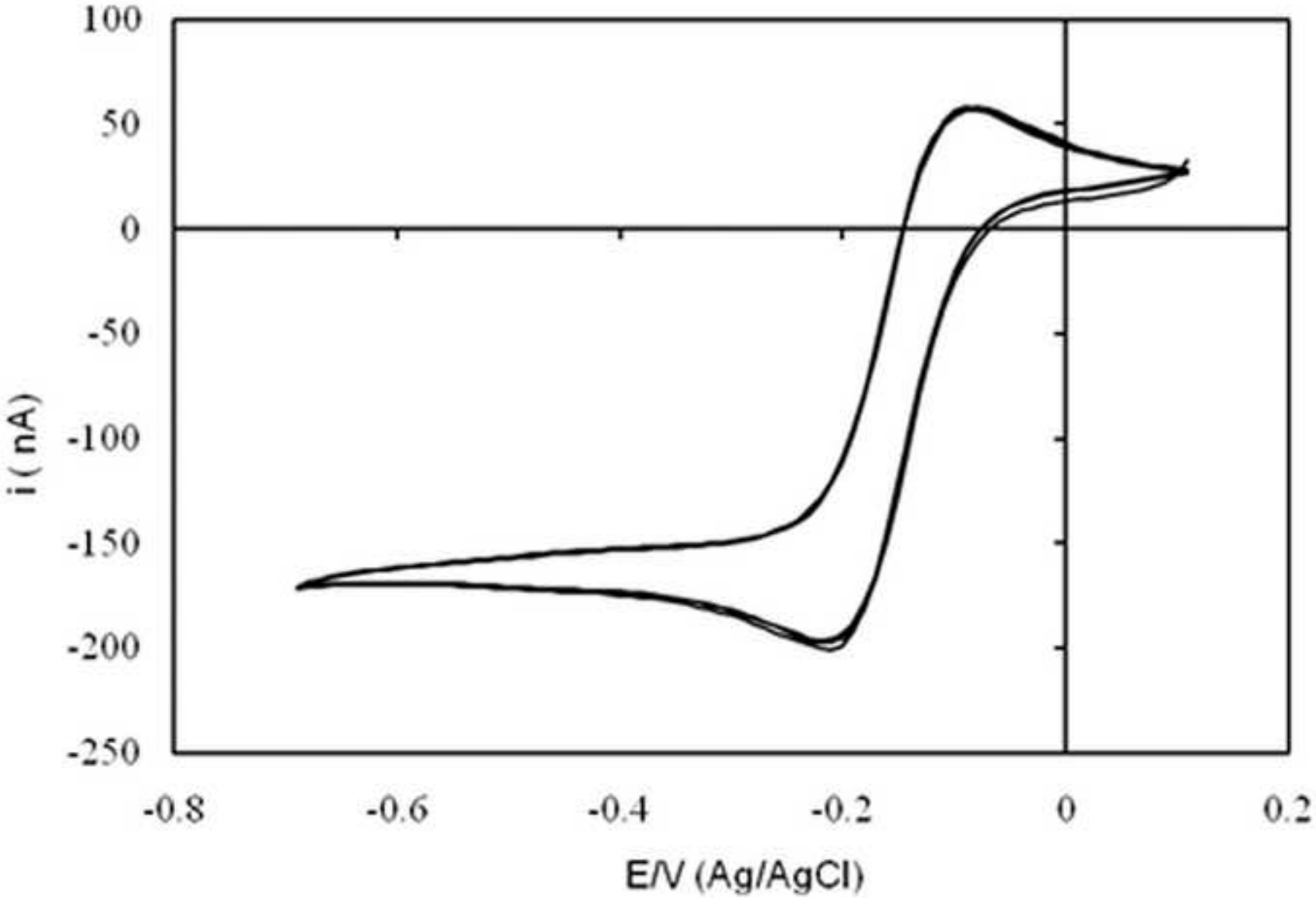

Figure 10
Click here to download high resolution image

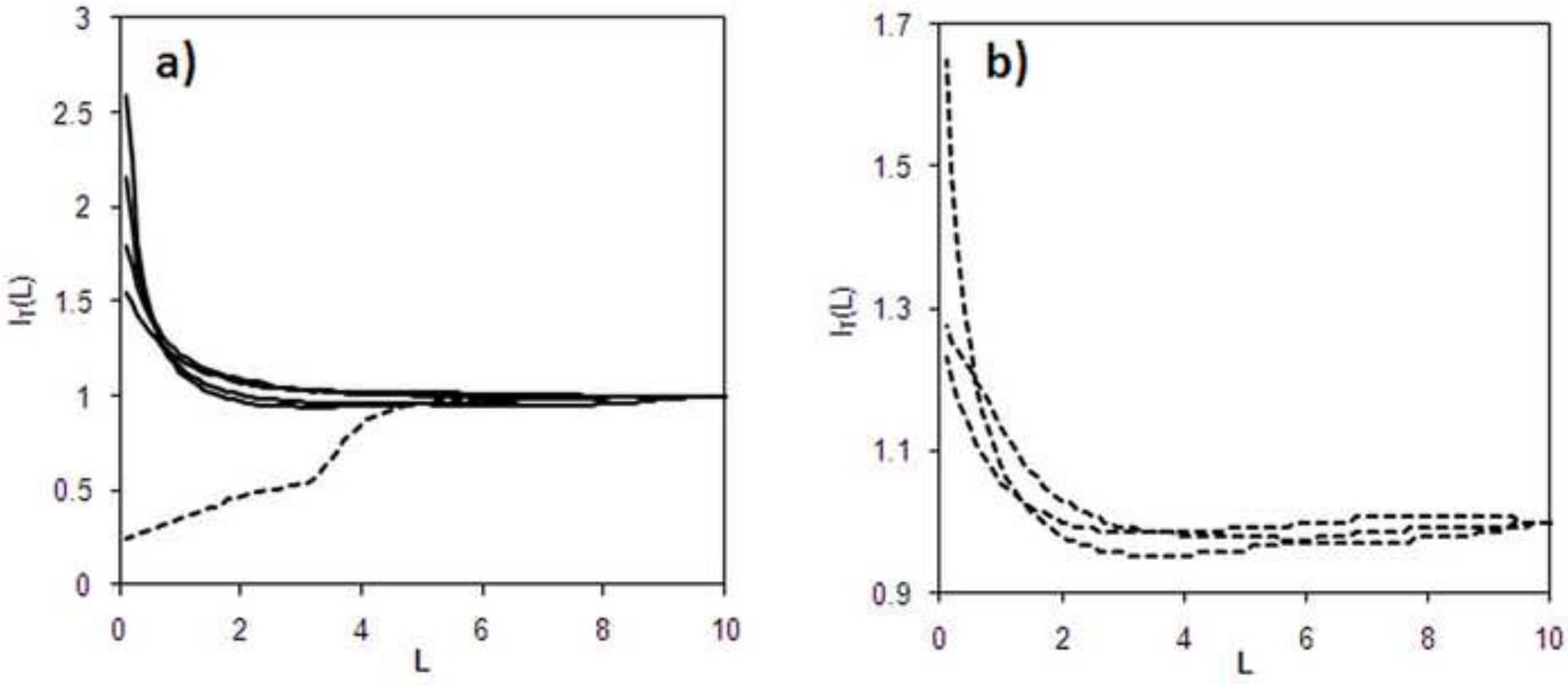

Figure 11

Click here to download high resolution image

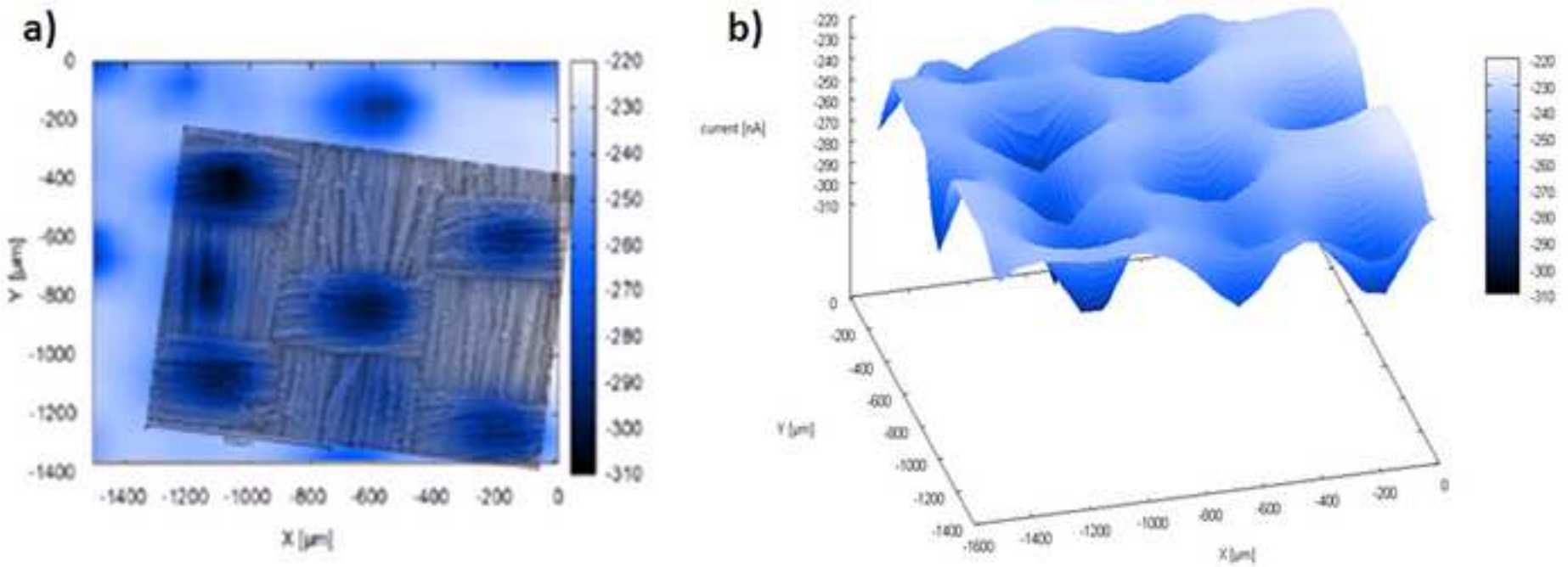

Table 1

Click here to download high resolution image

Sample	Chemical composition	Doping ratio N^+/N_{Total}
PES-PPy/$PW_{12}O_{40}^{3-}$	$C_{50}N(PW_{12}O_{40}^{3-})_{0.053}O_{0.60}$	0.196
PPy/ PPy/$PW_{12}O_{40}^{3-}$ + Pani/HSO_4^-/SO_4^{2-}	$C_{77}N(HSO_4^-/SO_4^{2-})_{0.210}$	0.224

Table 2

Click here to download high resolution image

	PES-PPy/$PW_{12}O_{40}^{3-}$	PES-PPy/$PW_{12}O_{40}^{3-}$ + Pani	Assignments
C1s	284.1	284.2	C-C/C-H
	285.6	285.8	C-N
	287.4	–	C=O
O1s	530.3	–	W-O-W
	531.7	–	W=O
	--	531.2	SO_4^{2-}
	--	532.8	HSO_4^-
N1s	--	398.8	-N=
	399.7	399.7	-NH-
	--	401.6	N^+
	401.9	–	N^{2+}